

Flexible electronics under strain: a review of mechanical characterization and durability enhancement strategies

K. D. Harris^{1,2} · A. L. Elias^{1,3} · H.-J. Chung³

Received: 14 September 2015 / Accepted: 6 December 2015 / Published online: 21 December 2015
© Her Majesty The Queen in Right of Canada 2015

Abstract Flexible electronics incorporate all the functional attributes of conventional rigid electronics in formats that have been altered to survive mechanical deformations. Understanding the evolution of device performance during bending, stretching, or other mechanical cycling is, therefore, fundamental to research efforts in this area. Here, we review the various classes of flexible electronic devices (including power sources, sensors, circuits and individual components) and describe the basic principles of device mechanics. We then review techniques to characterize the deformation tolerance and durability of these flexible devices, and we catalogue and geometric designs that are intended to optimize electronic systems for maximum flexibility.

Introduction

The development of flexible electronics has received considerable attention recently, as R&D efforts in this area are ultimately expected to facilitate extremely valuable device applications. Researchers are now frequently describing devices or techniques that pave the way toward conformable sensors for health-care applications, electronic skin for versatile and adaptable robots, or flexible

analogues of conventional consumer electronics such as e-readers, mobile phones, or televisions. Some recently published images representing a diverse range of these flexible devices are collected in Fig. 1.

Because the range of applications is extremely broad, device flexibility requirements are quite varied. In some cases, extremely high strain implementations are anticipated, including sensing/communications devices integrated directly onto skin or other organs (e.g. the devices in Fig. 1b, d) or electronics embedded into clothing or other textiles. In other applications, small but repetitive strain cycles are expected, while a different range of applications require tolerance of moderate one-time strains. Even if the electronics are intended to be used while firmly fixed in place, they must still be able to withstand various stresses and strains inherent to their manufacturing process or deployed location, such as bending deformation in a roll-to-roll manufacturing line, thermal expansions from variations in ambient temperature, or abrasion as a result of weathering or user handling. This evidence all points toward a need for high-quality R&D directed specifically toward improving the strain tolerance of electronic materials and devices.

Flexible devices must be capable of undergoing deformation and at the same time the functional properties and electronic performance parameters must be unaffected by the strain process. The electrical resistance of a flexible electrode, for example, should be low before, during and after a deformation cycle, while the power conversion efficiency of a flexible solar cell should be large throughout an entire strain process. Similarly, for devices that actively measure strains or harvest energy from strain (strain sensors and piezoelectric generators, for instance), the response to strain should be consistent throughout the entire device lifetime.

✉ K. D. Harris
ken.harris@nrc-cnrc.gc.ca

¹ National Institute for Nanotechnology, Edmonton, AB, Canada

² Department of Mechanical Engineering, University of Alberta, Edmonton, AB, Canada

³ Department of Chemical & Materials Engineering, University of Alberta, Edmonton, AB, Canada

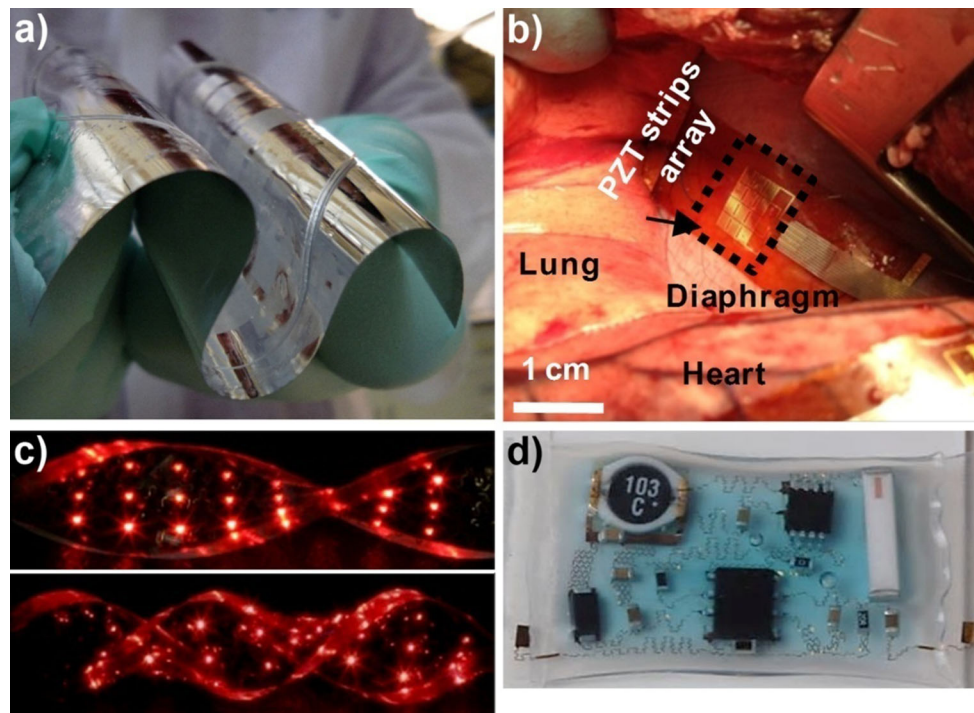


Fig. 1 Examples of flexible electronic devices, including **a** an array of flexible pressure sensors (reproduced with permission) [1], **b** a piezoelectric energy harvester integrated with a bovine diaphragm (reproduced with permission) [2], **c** a twistable LED array

(reproduced with permission) [3] and **d** a stretchable and skin-mountable physiological measurement device (reproduced with permission) [4]

It should also be noted that the term flexible can refer to tolerance of a range of different mechanical deformation modes. At the dawn of the research field, “flexible electronics” usually indicated bendable versions of planar electronics. More recently, foldable, stretchable and twistable modes have also been enabled through advanced device designs, with the current state-of-the-art represented by three-dimensional, non-planar geometries. All of these deformation modes are relevant to the present review, and we will use the term “flexible electronics” to broadly represent devices that accommodate any of these mechanical deformation modes. To evaluate flexibility or strain tolerance, researchers rely on a wide range of techniques such as cyclic testing in bending or stretching modes, scratch testing, or peel testing. Each of these characterization techniques reveals different information about the mechanical reliability of the materials and devices. It is the intention of this paper to review these test procedures and catalogue the progress researchers have made to maximize the durability of materials and devices as measured by each of these mechanical characterization techniques.

The review is organized as follows: we begin by surveying materials, devices and fabrication techniques to introduce the subject matter. Because considerable review material already exists in these areas, we provide only an

overview and, wherever possible, direct the reader toward additional information. We then outline basic concepts in mechanics that pertain to flexible or stretchable devices. We write to target the non-expert and provide the basis for understanding of the topics in subsequent sections. Following this, we review in detail the types of mechanical tests that are performed to evaluate the strain tolerance of materials and devices. We discuss the equipment required to perform each characterization process, and we overview measured results for a variety of flexible electronic devices (as organized by the mechanical characterization technique rather than by device type). Because mechanical measurements go hand-in-hand with efforts to improve device longevity, we also discuss ongoing research activities that are specifically directed toward improving the durability of flexible electronic devices.

Materials, applications and fabrication techniques

Conductors, semiconductors and insulators

The basic building blocks for electronic components are electrical conductors, semiconductors and insulators, and many research efforts have been made to identify flexible or stretchable materials in each of these categories [5].

Metals are the best known electrical conductors. In high-performance electronics applications, the conductivity of metallic films ($\sigma \sim 10^4 - 10^6$ S/cm) is highly advantageous (possibly even essential), and these materials are often capable of withstanding modest bending-mode deformations [6]. Metallic films can be applied and patterned either in a conventional process involving vapour deposition followed by photolithography [6], or by printing a nanoparticle-loaded ink and sintering to form an electrically continuous film [7, 8]. The key challenge in the latter case has been developing sintering conditions that are compatible with plastic substrates.

In applications demanding stretching or large-scale bending, however, metal films are often found to be mechanically inadequate [9–13], and this has led to the development of several alternative geometries and materials [14]. For instance, gallium/indium mixed in proportions near the eutectic point (known as eGaIn) is a metallic conductor that is also a liquid at room temperature [15]. Electrical conductors incorporating eGaIn or other liquid metals are capable of tolerating large deformations without suffering a noticeable loss of electrical conductivity [15–19], but on the other hand complex fabrication strategies are often required, and strain-tolerant encapsulation to prevent leakage is certain to be an issue.

Percolated networks of conducting nanowires (NWs) are also used to form strain-tolerant films for electronics applications. With this design strategy, large quantities of high-aspect ratio conductors are cast onto a substrate to form a continuous network that is either randomly arranged or guided with an aligning field [6, 20–22]. Junctions between NWs increase the electrical resistance of the network, but because free volume exists around the electrically conducting network, NW meshes are able to accommodate mechanical strain by hinging/sliding at points where individual NWs intersect one another [23]. These percolated networks also have the added advantage of redundant pathways for charge transport. If links are damaged within the conducting network, charge is redirected to neighbouring links without isolating large sections of the device. Electrically conducting films of this nature have been formed in a variety of materials including carbon nanotubes (CNTs) [6, 24, 25], silver nanowires [9, 26, 27] and copper nanowires [9, 28]. A comprehensive review of this topic is given in a recent publication by Yao and Zhu [29].

Polymeric materials that naturally have some degree of mechanical compliance can also be employed to form strain-tolerant electrical connections. Several strategies are available to ensure both electrical conductivity and mechanical durability coexist in the same material. These include loading a mechanically compliant, non-conducting elastomer with electrically conducting fillers such as metals

or carbon [10, 11, 30–32], or choosing, and appropriately doping, a π -conjugated polymer [9, 33–35]. The first approach has a long history, with the concept of “conductive rubbers” dating back to the 1950s [32]. The modulus of these composites can be predicted using models such as the Halpin–Tsai model [36, 37], taking into account the mechanical properties of both the matrix and filler materials, the volume fractions, the filler dispersion, the shape of filler particles and the alignment of filler within the matrix. With sufficient loading (i.e. above the percolation threshold), the fillers (most commonly carbonaceous particles) tend to dictate the electrical properties of the composite. Numerous applications of these conducting composites have been identified including dissipation of static charge and electromagnetic interference shielding; however, the conductivity of carbon-filled rubbers has historically been too low (<0.1 S/cm) for most electronics applications [10]. With the development of nanofillers such as carbon nanotubes or other NWs, however, reduced loading is often required to achieve percolation, and conductivities in excess of 100 S/cm are now being measured [10].

Conjugated polymers such as polypyrrole, polyaniline or polythiophenes are also used in flexible electronics applications [9, 11, 33–35, 38–40], and in many cases composites (conducting polymers loaded with nanotubes, for instance) are also formed to further tailor mechanical or electrical properties [11]. Presently, the key organic material is the polythiophene derivative poly(3,4-ethylenedioxythiophene):poly(styrenesulfonate), or PEDOT:PSS [41]. This material is typically cast from an aqueous suspension, and additives including small polar molecules or surfactants have been included to improve conductivity [9]. The best conductivities attained with these materials are greater than 1000 S/cm, and processing is performed from solution, which is an advantage when high-volume manufacturing is considered. On the other hand, it is important to be aware that the use of polymeric materials does not necessarily ensure favourable mechanical properties, and moreover conducting polymers do tend to have considerably lower electrical conductivity and stability than metallic conductors [25].

Graphene has also been utilized as an electrical conductor in applications requiring mechanical deformations [24, 42]. The material is intrinsically strong and flexible [43], and it has fairly low resistance in an undoped state (~ 6 k Ω/\square for an undoped monolayer). The conductivity can, moreover, be further improved through electrostatic or chemical doping to increase the charge carrier concentration. The highest performance graphene tends to be produced by mechanical exfoliation of bulk graphite or in chemical vapour deposition reactions. The former, however, is not considered to be easily scalable to high-volume

manufacturing, while the latter is not directly compatible with plastic substrates and requires a transfer step [44]. An alternative, high-volume technique that may be advantageous for flexible electronics applications is chemical synthesis and printing directly from solution [45].

Transparent conductors make up an important subset within the materials for flexible electrical conductors [9, 25, 46–49]. All of the mechanical and electrical requirements for flexible conductors must still be satisfied, while provisions for light transmission must also be engineered into the material [25]. The spectral range for transparency is determined by the intended application: for example, displays require good transparency across the wavelengths visible to the human eye (400–700 nm), whereas solar cells require broader transparency as weighted by the power of the solar spectrum and the absorbance of the photoactive layer. Thin metal films, conductive rubbers and most π -conjugated polymer systems tend not to meet the necessary performance standards for transparent conductors, while graphene, several percolated NW systems and PEDOT:PSS appear to be well suited. At present, the materials most commonly used in these applications are the transparent conducting oxides (TCOs) such as indium tin oxide (ITO) [47, 48]. These materials are well known to be quite brittle, but in applications requiring only moderate flexibility, the device geometry can be designed to allow TCOs to be included.

Many of the strategies used to fabricate flexible or stretchable conductors can also be adapted to form flexible semiconductors [9, 11, 20, 21, 46]. Both semiconducting NWs [22, 46, 50] and semiconducting organics (polymers and small molecules) [11, 35, 38, 39, 51, 52] have been synthesized and cast from solution for flexible electronics applications. The carbon nanomaterials (graphene and CNTs) have also been used successfully, although in this case it is often necessary to include a dedicated processing step to ensure semiconducting behaviour (e.g. removing metallic CNT links) [6, 24, 42, 53]. Despite this range of materials, the formation of deformation-tolerant semiconductors with good electronic properties does tend to represent a considerably more difficult problem than the formation of strain-tolerant conductors. Even organic semiconductors often degrade markedly under strain [54, 55], and some results reveal correlations between charge carrier mobility and elastic modulus [56], or solar cell performance and elastic modulus [57]. This behaviour is thought to be mediated by molecular order and crystallinity, which generally facilitate good charge carrier mobility while simultaneously stiffening the materials. This implies that flexibility and favourable electronic properties are inversely related for organic semiconductors [58, 59]. It is also notable that conventional semiconductor materials, such as silicon or III–V materials, have been

revisited as key components for flexible electronics. Their utilization is usually accompanied with advanced designs that will be discussed later in the review. Also, in the case of flexible solar cells, perovskites are particularly important light-absorbing semiconductors [60, 61].

Flexible insulators tend to be discussed less often in the literature than conducting or semiconducting counterparts, but they are no less critical to the successful operation of several electronic devices. Because field-effect transistors (FETs) demand the most specific functional properties, flexible insulators are usually reviewed in the context of these FET applications [6, 24, 51]. From this standpoint, an ideal insulator is mechanically compliant, can be deposited at low temperature without vacuum techniques, has a large dielectric constant (κ) and forms a continuous, pinhole-free dielectric at low thickness. The ceramic oxides such as SiO₂ and the “high- κ ” dielectrics, ZrO₂, TiO₂, HfO₂ and Al₂O₃, developed for conventional rigid electronics generally achieve the best electronic performance, but they also tend to be brittle. In applications requiring only modest flexibility, devices incorporating these oxides can achieve acceptable flexibility with careful design of the geometry, but if large, repeated deformations or stretchability is necessary, then polymeric dielectrics are generally employed. Many polymeric materials can be deposited from solution by spin-coating or printing, and inexpensive materials such as polydimethylsiloxane (PDMS), polymethylmethacrylate (PMMA) or polyimide (PI) have been successfully used in FET applications. Another material, parylene-C, can be deposited from the vapour phase, forming highly conformal coatings. Because polymers with various chemical compositions are available, the designer can exercise considerable freedom in choosing organic insulators with the best possible compatibility (i.e. solubility, wettability, thermal behaviour, etc.) with other materials in the device stack. Hybrid gate insulators that include both high- κ oxides and polymers have also been demonstrated on plastic substrates, and the associated FET devices had excellent electronic properties coupled with flexibility [62].

Not to be neglected, barrier layers are often included in flexible electronics systems to prevent diffusion of gases into the device and the associated degradation of the electronic materials [63]. Often encapsulating the electronics system, these materials can be subjected to high strain and/or abrasion and must be carefully chosen to withstand their mechanical environment.

Substrates

Substrates are also a critically important consideration as their mechanical properties can dominate those of the integrated system. The materials can generally be grouped

into three broad categories: plastic films, metal foils and fibrous materials (including paper and textiles).

Plastic films are the most common flexible substrates noted in the literature [9, 11, 64–70]. Properties vary considerably from material to material, but in general plastic films tend to be relatively inexpensive and lightweight, making them well suited to high-volume manufacturing. Some key materials include polyethylene terephthalate (PET), polyethylene naphthalate (PEN), polycarbonate (PC), polyethersulfone (PES), polyimide (PI) and polyarylate (PAR); many other options are also available as necessary. Because the material properties vary greatly, it is important to consider thermal stability, mechanical stability, solvent resistance, surface energy/wettability, diffusivity, optical clarity, surface smoothness and cost to effectively guide the selection of substrates for any given application [70]. A good discussion of processing temperatures can be found in the review by Fortunato et al. [65]. This publication also discusses the important issue of device deformation induced by mismatching coefficients of thermal expansion for plastic substrates and typical device materials.

In applications where stretchability is important, most of the materials noted above are abandoned in favour of highly compliant elastomers such as polydimethylsiloxane (PDMS), polyurethanes, or the multiblock copolymer styrene ethylene butadiene styrene (SEBS) [9, 11, 71]. Cotton et al. demonstrated that the mechanical properties of PDMS could be photopatterned to locally soften the substrate in regions intended to support interconnects rather than rigid components [72]. In another interesting approach, stretchable devices were also formed on non-elastomeric substrates by cutting a strain-relieving pattern into the substrate [73]. With these perforated substrates, hole shape dynamically varies to accommodate tensile strain.

Metal foils are commonly introduced when high-temperature processing is a requirement [64, 66, 68]. As substrates, metals tend to be relatively temperature resistant, and they are also excellent electrical and thermal conductors, good barriers against the diffusion of water and oxygen, and relatively resistant to most solvents. Stainless steel represents the leading material, but other options (such as titanium or copper foils) are also available if particular attributes of these metals are advantageous. The weight of metal foils is a key disadvantage, and the materials also tend to be more expensive and less flexible than plastic substrates.

Due to its extremely low cost, many researchers also endeavour to use paper as a substrate for electronic components and circuits [33, 74, 75]. Paper is inexpensive (~ 10 ¢/m²), even when compared against commodity plastics such as PET (~ 2 \$/m²). Bulk paper does,

however, have a range of drawbacks when electronics applications are considered: water and other solvents can be absorbed by the material and may affect the electronic components, the surface is generally rough making device fabrication challenging, and light scatters from surface irregularities which may rule out some applications. Most of these issues can be addressed with chemical treatments, but these treatments do add cost to the manufacturing process. Nevertheless, the potential for extremely low-cost manufacturing means that paper cannot be discounted as a substrate material.

Many of the challenges associated with paper substrates also extend to devices intended to be integrated with clothing or other textiles [75–80]. Economically, these substrates are important as the market for clothing with integrated electronics is ultimately expected to be large. Researchers are, however, facing numerous challenges. For example, textiles are composed of numerous individual fibres, making fabrication of surface-mounted devices difficult, and most textiles are also capable of transmitting air and absorbing large amounts of water which can affect electronic components both chemically and mechanically. Typical human interactions with clothing are also important: the clothing must be washable, and the integrated electronics should be sufficiently compliant that they not only survive mechanical deformation, but feel comfortable to the wearer (imagine sitting on a fold). One useful advantage of textiles with respect to the integration of electronics, however, is that fibres themselves can be rendered electrically conducting by blending in conducting components [75, 78, 81].

Applications: discrete devices and integrated systems

Using the set of basic materials described above, a wide array of passive and active flexible electronic components may be fabricated, and these discrete devices can be arranged to form power supplies, sensing platforms or complete electronic systems. Flexible thin-film transistors (TFTs) are key components in many of these systems, and generally field-effect transistors that are utilized in contemporary applications [6, 21, 24, 46, 65, 66, 82–85]. In the most common implementation, FETs are three-terminal devices that operate based on modulation of the electrical conductivity in a patterned semiconductor “channel”. Electrical current is injected into and extracted from the channel at high-conductivity electrodes denoted the “source” and “drain”, while the conductivity of the channel is determined by the voltage at a “gate” electrode. The gate is separated from the source, drain and channel by a “gate insulator”, but it is capacitively coupled to the channel such that the concentration of charge carriers in the

channel is directly tied to the gate voltage. Varying this voltage, therefore, adjusts the current flowing between source and drain. These devices act as switches or amplifiers in electrical circuitry, and stimulus-responsive gates can also form the basis of sensing devices. Some of the key parameters that describe FET performance are the charge carrier mobility (μ), ratio of currents in the on/off states ($I_{\text{on}}/I_{\text{off}}$), threshold voltage (V_{th}) and the “subthreshold slope” which describes how readily the device switches between on/off states in response to small variations in gate voltage. In a deformation-tolerant TFT, the high-conductivity electrodes, the semiconducting channel and the gate insulator must all be capable of withstanding mechanical deformation. Generally, flexible FETs based on inorganic semiconductors, including silicon, have the best measured electronic performance parameters, although steps must be taken to ensure that deformation tolerance is acceptable and fabrication temperatures are compatible with flexible substrates [46, 65, 82, 86, 87]. Devices based on both organic materials [51] and carbon nanomaterials (CNTs and graphene) [6, 24] have also been fabricated, but in the former oxidation-induced degradation is problematic and performance metrics tend to be lower than for inorganic materials, while in the latter achieving appropriate electronic properties (i.e. separating semiconducting from metallic CNTs, or engineering graphene with an appropriate bandgap) can be challenging.

Memory elements are also critical components of many electronic devices, as they are used to store data and programming information. High-value consumer products such as televisions, mobile phones and e-readers incorporate memory, and therefore flexible versions of these products will ultimately require flexible memory devices to be developed. Many types of memory elements are available, and it is beyond the scope of this review to describe the operating principles for the various classes. This information was thoroughly reviewed by Han et al. [88], and the authors also provide considerable information on progress toward developing flexible memory elements. Some of the key issues include developing low-temperature processing conditions that are compatible with flexible substrates, adding appropriate planarization layers to reduce the influence of substrate roughness, and ensuring that process solvents do not damage the substrate or other layers of the device stack.

Integrating lighting with electronic circuitry allows active displays to be formed, and many research advances leading toward the creation of flexible displays have also appeared in the literature. Light-emitting diodes (LEDs) are the components most commonly suggested as lighting elements for flexible displays (and also for other applications such as automotive lighting and biomedical imaging). In effective devices, LEDs should retain a fixed emission

wavelength under strain, and efficiency (W/W) should remain high through repeated deformation cycles. Research efforts to fabricate these flexible LEDs have been ongoing for several years, such that several reviews on flexible electronics have incorporated sections devoted to lighting [6, 10, 21, 39, 89, 90].

Another focus area for flexible electronics is fabrication of devices for energy generation and storage, including solar cells, energy scavengers, batteries and supercapacitors. Solar cells (or photovoltaic devices) generate electrical current in response to light absorption at a photoactive semiconductor [9, 39, 66, 68, 91–95]. Provided that the photon energy exceeds the semiconductor bandgap, light striking the semiconductor excites electrons from their ground states, generating both negative and positive charge carriers (i.e. electrons and holes). To make up an electrical current, these carriers are shunted to opposite faces of the solar cell and extracted through electrodes, one of which must be transparent in order to admit light into the cell. Conventional photovoltaics (e.g. silicon) include a p - n junction to efficiently separate charge carriers [96], whereas organic photovoltaics use a chemical potential for this purpose [93]. The key performance parameter is the power conversion efficiency (PCE), and subsidiary metrics include the short circuit current density (J_{SC}), open circuit voltage (V_{OC}), fill factor (FF), series resistance (R_{S}) and shunt resistance (R_{SH}). A flexible solar cell must retain high PCE throughout repeated deformation cycles, and incorporate robust electrodes, semiconductors, interfacial modifiers and wiring. A subclass of solar cells, the dye-sensitized solar cells (DSSCs), also tends to include liquid electrolytes for charge transfer, and these must also be effectively contained during strain cycling [68, 92].

Batteries and supercapacitors are both energy storage devices [33, 34, 75, 95, 97–100]. In a battery, energy is stored electrochemically, and charge carriers are released through distinct chemical reactions. Lithium-ion batteries [98, 99, 101] currently dominate the market with the vast majority of portable electronics now powered with this battery type. Li-ion batteries incorporate a lithium compound as a cathode and carbon as an anode and often high-surface area “charge collectors” are also included at the electrodes. Electrical current is composed of Li^+ ions moving between these electrodes through an electrolyte medium and charge separator membrane. In direct contrast with batteries, supercapacitors store energy electrostatically and chemical reactions are not involved in charge cycling. This is advantageous in that charging/discharging is fast, and degradation with charge cycling is generally not severe. Key performance parameters for each of these devices are energy density (in Wh/g), power density (in W/g), capacity (in Ah/g, which is a function of discharge rate) and cycle life (which is the number of charge/

discharge cycles that can be sustained before the capacity falls below some critical value, usually 80 %). Batteries tend to have lower production cost and considerably better energy density than supercapacitors, while supercapacitors have superior power density and cycle life. Some of the key issues faced in developing flexible batteries and supercapacitors include reliably encapsulating liquid electrolyte or developing high-performance solid-state electrolytes, identifying deformation-tolerant electrode materials/architectures, and integrating these constituent materials into a reliable high-performance device [75, 97–99, 102].

Energy scavenging from mechanical vibrations has also been suggested as a potential power source for flexible electronics. In energy scavenging devices, piezoelectric structures transduce mechanical strain into electrical charge, and many efforts have been undertaken to identify promising materials and architectures that maximize power output [103, 104]. Critical performance parameters include the piezoelectric charge constants, d_{ij} (units: m/V), which describe the voltage generated along axis i in response to strain along axis j . One of the key technical issues is that the mechanical strains required to generate useful power output often exceed the fracture limits of the brittle piezoelectric structures.

Another useful class of devices that is expected to be integrated on deformable substrates are sensing elements, including chemical sensors, temperature sensors and pressure/strain sensors. Chemical sensors are already widespread, but fabricating analogues on compliant substrates may lead to implantable devices with improved biocompatibility or wearable monitoring systems. Because the range of possible analytes is enormous, the operating principles for this class of devices are also quite diverse [11, 103, 105]. The most common mechanism is chemically modulated resistance measurement in a semiconducting material, and the associated challenge is the fabrication of high-quality semiconductors on temperature-sensitive plastic substrates. To address these issues, nanomaterials or organic semiconductors are often used as sensing elements, and transfer steps can be included in the fabrication process.

Pressure/strain/tactile sensors are, in one important manner, quite different than the remainder of the devices discussed in this review. Rather than simply tolerating deformation, most of these devices actually incorporate deformations as a part of their operating mechanisms. The operating principles within this class of devices are also quite varied, but the technologies have been grouped into several categories (piezoresistive devices, capacitive devices, piezoelectric devices and optical devices). An excellent review by Bao et al. [106] and several other reviews include sections devoted to pressure or strain sensors [11,

91, 103]. Because the devices operate by various mechanisms and incorporate a variety of materials, it is difficult to broadly define the technological challenges for the entire class of devices. The applications do, however, all require devices that are able to endure repeated strain cycling, and therefore mechanical testing to gauge deformation tolerance (e.g. tracking the evolution of sensitivity during strain cycling) is vital for essentially any pressure/strain sensor or any other deformable sensing platform.

Advances in flexible electronics have also enabled the development of a wide range of new bionic devices that could not be realized using rigid materials [66, 76, 79, 107–111]. External to the body, flexible electronics have been engineered to conform to the skin and form the basis of a variety of flexible physiological detectors [107, 112–121], such as sensors of hydration, pulse, oxygenation or electrophysiological signals. With parallelization, sheets of these miniaturized, conformal and addressable sensors have been integrated to form “electronic skin” that may allow robotics or prostheses to sense their surroundings with fine resolution [11, 106, 122–126]. Within the body, flexible electronic devices are also being investigated as neural interfaces for mapping brain activity [109, 127], restoring motor function by stimulating spinal neurons [109, 128] or restoring vision in the eye [129]. Sophisticated, flexible implants have also been used to map other phenomena in vivo, such as a flexible, elastomeric heart sock that includes an integrated electrocardiogram and sensors for pH, temperature and strain [130].

In these biomedical applications, the electronics are generally expected to be fabricated ex situ on a substrate chosen for compatibility with the fabrication processes, then installed on the target tissue (with or without a permanent backing) [108, 130]. Once the electronics are in place, two key issues for both skin-mounted and implanted devices are ensuring the stability and biocompatibility of all materials, particularly if long-term use is intended [131]. For example, the mechanical mismatch between conventional (i.e. rigid) electronic materials and soft biological tissue often leads to irritation during motion (either macroscopic movements of the body or local micromotion due to blood pulsation) [132]. The mechanical mismatch is also theorized to promote glial scarring and contribute to the foreign body response of biological tissue to implants. For some devices, such as brain–computer interfaces which aim to measure or transmit electrical signals, these electrically insulating scars are considerable obstacles to device functionality [133–135]. Because each type of biological tissue has different characteristics, design constraints built around stability and biocompatibility tend to be heavily application specific, but in general devices based on flexible materials are expected to have considerably improved biocompatibility.

Fabrication techniques

Flexible or stretchable electronic devices are fabricated with a wide array of techniques. Exploratory studies involving either new materials or new applications for established materials are usually performed by fabricating simple devices with modest dimensions and using low-volume fabrication techniques. For example, electrical conductors are deposited by physical vapour deposition (PVD) processes (i.e. evaporation or sputtering) [136], and they are patterned by shadow-masking or simple optical lithography [136]; semiconductors are spin-cast from solution if an appropriate solvent can be identified [38], or they are deposited in PVD or chemical vapour deposition (CVD) [136, 137] processes; and insulators are spin-cast from solution or deposited by PVD. In some instances, spin-coating is substituted with techniques such as drop-casting, bar-coating or guided assembly [21], and evaporation/sputtering processes are replaced with casting of metallic inks, CVD, or atomic layer deposition (ALD) [138, 139].

These techniques are extremely useful for screening materials, and the equipment required to perform these basic processes are staples of most research labs specializing in flexible electronics. In the long term, however, the fabrication process truly capitalizes on the potential for low-cost fabrication by introducing high-volume manufacturing techniques in a continuous roll-to-roll (R2R) process [38, 140–143]. Evaporation, sputtering and CVD have long been R2R compatible [144–148], although the high temperatures generally associated with CVD reactions make development of processing conditions compatible with plastic substrates more challenging than in analogous processes on rigid substrates. Considerable effort has also been directed toward designing ALD reactions that are R2R compatible [149]. Another staple of high-volume manufacturing is the set of printing techniques, which can be sub-divided into two categories: master-printing and digital printing [140]. The master-printing techniques require a pre-patterned printing plate as a master and include the following: flexography (i.e. relief printing) in which ink is transferred to the substrate from protruding features in a relief plate; gravure printing (also known as intaglio printing) in which ink is transferred to the substrate from the wells in the relief master; offset printing (also known as planographic printing) in which ink is transferred from a fully planar master that selectively collects ink according to an oleophobic versus oleophilic surface pattern; and screen printing in which ink is pressed through a patterned screen to make an image on the substrate. Digital printing techniques do not require a master, as they are instead based upon relative motion between a substrate and

a printing head or nozzle. Inks are dispensed through the nozzle, and because this relative motion can easily be reprogrammed, the digital printing techniques tend to be highly adaptable. The digital printing techniques include (among others) inkjet printing [7, 150, 151], direct ink writing [152, 153] and laser patterning, in which ink is selectively transferred to a substrate based on local heating from a laser [154, 155]. Other roll-to-roll compatible techniques include knife-over-edge coating [141, 142], slot-die coating [141, 142] and electrospinning [21, 156, 157], in which a viscoelastic jet is drawn from a polymer blend and cast on the substrate.

As opposed to the conventional semiconductor industry, the fabrication challenges in flexible electronics are not primarily in miniaturizing devices, but in adapting to deformation and instability of the substrate [65, 70, 140, 158, 159]. If devices cannot be fabricated directly on the target, another manufacturing option that is available is “transfer printing” in which materials or complete devices are pre-fabricated on a convenient substrate before they are harvested and transferred to a flexible target as if they were “inks” [6, 20, 44, 83, 107, 160, 161]. This technique, which resembles pick-and-place methods, is relatively young, but may ultimately be used to form high-quality inorganic devices with cost-effective R2R fabrication.

Mechanics and modelling

Basic material properties

To understand the mechanics of devices under deformation, it is first important to define some basic parameters. Strain is a unitless quantity describing the physical deformation of a shape, and adjectives are often added to further specify the nature of strain: for example, tensile strain describes a shape elongated with respect to reference dimensions, compressive strain describes a compacted shape, and shear strain describes a deformation in which parallel planes within the sample are translated in-plane with respect to one another. Compressive, tensile and shear strains are graphically depicted in Fig. 2 along with the applied forces that produce these deformations.

The typical mathematical representation of tensile or compressive strain, ε , is provided in Eq. (1), where L_0 is the original dimension and ΔL is the change in dimension with respect to this reference state. In tension, a shape that doubles in length has reached $\varepsilon = 1$, while in compression a shape that is half its original length has reached $\varepsilon = 0.5$. By necessity, shear strain, γ , is defined differently and as shown in Eq. (2), the tangent of the strain angle is used for this purpose.

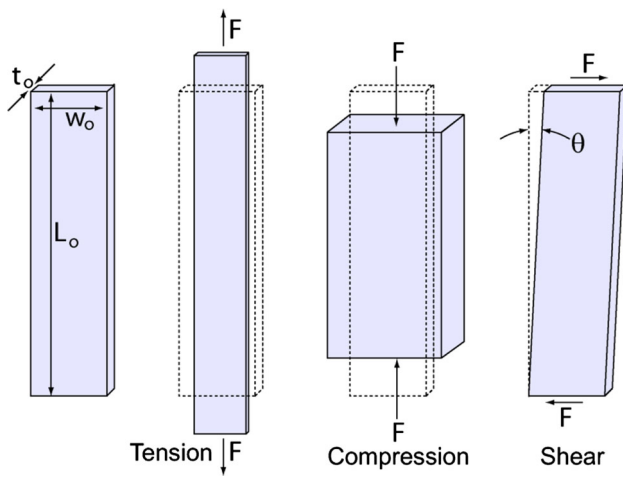


Fig. 2 Simple drawings of forces and deformations in tension, compression and shear. Forces are denoted F ; original dimensions are denoted L_o , w_o and t_o ; and the shear strain angle is denoted θ

$$\epsilon = \Delta L/L \tag{1}$$

$$\gamma = \tan \theta \tag{2}$$

Stress is a measure of the internal forces distributed throughout a material, and it carries the units of pressure, Pa. The source of stress is often an externally applied load, but purely internal mechanisms (e.g. thermal effects, variations in composition, etc.) may also lead to considerable stress in the absence of external forces. Equation (3) describes a common situation for stresses generated during tensile or compressive experiments, and in the equation σ is the stress, F is the total applied force (usually measured in N), and A is the cross-sectional area of the sample (which has units of m^2 and is itself the product of thickness and width for rectangular samples). In shear, the mathematical definition of stress [shown in Eq. (4)] is similar, except that the symbol used to represent the stress, τ , has been substituted to clearly distinguish shear stress from tensile/compressive stress. It is important to note that non-uniformities in the sample (e.g. cracks, scratches, particulate, necks, edges, etc.) tend to localize stress, so the stress distribution is not necessarily homogeneous throughout the sample or throughout the experiment. Because these variations can have a significant effect on measured properties, most testing standards (including those prescribed by the ASTM) require that mechanical measurements should be repeated numerous times, and the results averaged.

$$\sigma = F/A \tag{3}$$

$$\tau = F/A \tag{4}$$

The basic material properties that describe the mechanical behaviour of a device under varying stress/strain conditions include (among many others) elastic

modulus, Poisson’s ratio, thermal expansion coefficient and toughness. The elastic modulus, E , relates stress to strain by the simple ratio shown in Eq. (5); however, the modifier “elastic” does imply that the stress and strain are only measured within the linear elastic (i.e. reversible) regime for the material. Beyond the elastic limit, a modulus may still be measured and reported, although it is very likely to differ from the elastic modulus as measured at low strain. For viscoelastic materials (e.g. polymers), the strain rate can also affect the measured modulus (with slower strain rate usually yielding lower modulus). In general, a large modulus indicates a stiff material, while a smaller modulus describes a more compliant material [14]. It is, however, quite important to note that the concept of “stiffness” as intuitively understood (i.e. “how hard is it to stretch or bend this?”) is not described exclusively by the modulus. The stiffness, k , carries units of (N/m) and is dependent on sample geometry in addition to modulus. Equation (6) is valid for a sample that is uniform perpendicular to an applied force, and it indicates that the stiffness scales linearly with both modulus and cross-sectional area. Implementing ultra-thin layers is therefore one approach that can be utilized to reduce the stiffness of a material.

$$E = \sigma/\epsilon \tag{5}$$

$$k = F/\Delta L = E \cdot A/L \tag{6}$$

Poisson’s ratio, ν , is the ratio of transverse strain to axial strain; it describes how a sample becomes thinner and narrower as it is stretched in tension, or expands as it is uniaxially compressed. A sample with $\nu = 0$ can be deformed in one dimension without affecting the other dimensions whatsoever, while a sample with $\nu = 0.5$ retains fixed volume during deformation (i.e. it is “incompressible”). For most materials of relevance to electronics, Poisson’s ratio varies between 0.2 and 0.5, with the elastomers such as PDMS having values near 0.5, many metals with values in the range 0.25–0.35, and typical ceramics in the range 0.2–0.3 [162]. In choosing materials for flexible electronics, it is important to match ν across material interfaces wherever possible, because at any interfaces where mismatches exist, the induced stress can lead to device failure by delamination [163, 164].

The coefficient of thermal expansion (α , units K^{-1}) describes dimensional changes in response to temperature variations. The coefficient of thermal expansion becomes a critical design parameter when high-temperature processing is required in the fabrication process [65]. For example, if a film is applied to a substrate at an elevated temperature, any appreciable α mismatch between film and substrate leads to the generation of biaxial interfacial stress as the temperature is returned to ambient [165, 166]. For a film on a rigid wafer, this stress forces the substrate to assume a

dome shape described by the Stoney equation [167]. On the other hand, for compliant substrates that are amenable to flexible electronics, interfacial stress tends to promote cylindrical rolling [65, 166], with radius of curvature, R , described by [168]

$$R = \frac{E_s t_s^2}{6(1-\nu)(\alpha_f - \alpha_s)\Delta T E_f t_f} \left[\frac{\left(1 - \frac{E_f t_f^2}{E_s t_s^2}\right)^2 + 4 \frac{E_f t_f}{E_s t_s} \left(1 + \frac{t_f}{t_s}\right)^2}{\left(1 + \frac{t_f}{t_s}\right)} \right] \quad (7)$$

In Eq. (7), the subscripts “f” and “s” indicate, respectively, the parameters associated with the film and substrate, t and ΔT represent, respectively, thickness and the change in temperature, and the Poisson’s ratio (ν) is assumed to be the same for film and substrate. The temperature-induced curvature, together with the tendency of typical substrate materials to shrink at moderate processing temperatures, has the potential to lead to overlay errors as different layers in a device stack are deposited [65, 166].

Toughness quantifies a material’s ability to resist failure. It is measured by integrating the stress–strain curve between zero strain and the strain at failure, and the units describe the quantity of energy absorbed at failure per unit volume, or (J/m^3) [162]. “Fracture toughness” is an entirely distinct parameter that describes a material’s resistance to crack propagation and brittle fracture. It is also closely related to “tear-resistance”, which is a key characteristic in the longevity of thin, sheet-like flexible electronics. The presence of cracks leads to local concentration of stress at the crack tip, and a “stress intensity factor”, K (units $\text{MPa m}^{1/2}$), relates applied stress to the concentrated stress at the crack tip. Unstable crack growth occurs when K reaches a critical value, and the magnitude of this critical value is the fracture toughness, K_c . Metals tend to have good fracture toughness ($>20 \text{ MPa m}^{1/2}$) and generally fail by ductile fracture, while oxides ($<5 \text{ MPa m}^{1/2}$) and glassy polymers ($<2 \text{ MPa m}^{1/2}$) have low fracture toughness and tend to fail by brittle fracture [162].

Finally, it is important to note that most mechanical parameters are not actually fixed quantities, but instead variables that respond to a wide range of conditions. All of the parameters noted above, for instance, are temperature dependent, and many parameters also vary with strain, strain rate, strain history, thermal history and composition of the environment. Small sample-to-sample variations can also lead to differences in measured properties, and therefore testing of multiple samples is typically recommended.

Film failure by cracking or delamination

The durability of flexible electronic devices under strain depends strongly upon crack formation/propagation [63,

169] and interfacial delamination [170], as these are the two key mechanisms by which devices fail in response to mechanical deformation. Examples of failure under each mechanism are shown in Fig. 3a, b. Cracks form and grow in order to relieve stress, and because coatings cannot be optimized solely based on load-bearing capacity, cracks typically develop in the functional coatings well before the substrate fails [171]. Crack evolution is usually measured by straining a sample under uniaxial [63, 169] or, less-commonly, biaxial [165] tension while observing through a microscope. In general, the progression for a rigid film on a

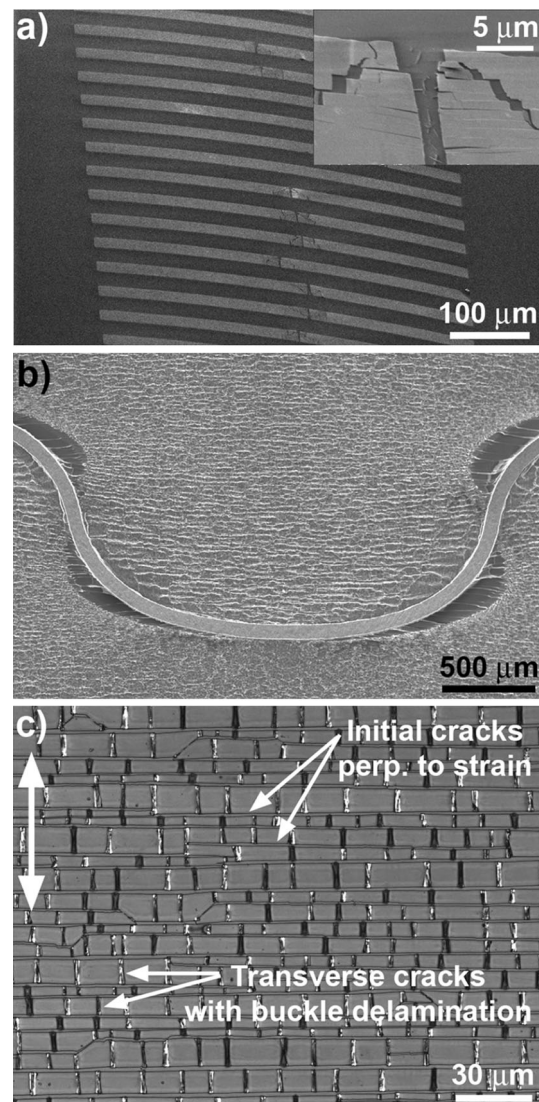


Fig. 3 Typical failure modes for flexible/stretchable electronics subjected to large or repeated mechanical strain include **a** cracking and/or **b** debonding. Reproduced with permission from (a) [182] and (b) [183]. In **c**, a large-area ITO film on PET is shown after uniaxial tensile strain to $\epsilon = 0.3$ (direction noted by *double-headed arrow on left*) and associated Poisson’s compression

more compliant substrate is crack initiation, crack propagation and crack densification (which includes a steady reduction in crack spacing until saturation), followed by transverse crack formation [172, 173]. A key measured parameter is the crack onset strain or critical strain (ϵ_{CO}), which tends to decrease with increasing film thickness, t [63, 174]. This behaviour is a result of the increasing energy release rate with increasing film thickness, and the classical scaling relationship has ϵ_{CO} varying with $t^{-1/2}$ [63, 171, 175]. For brittle materials on more compliant substrates (representing the vast majority of materials systems for flexible electronics), cracks tend to initiate around defect sites associated with surface irregularities in the plastic substrate [63, 169]. This effect is generally attributed to the concentration of stress at these surface defects, and therefore increased ϵ_{CO} is often observed for substrates with planarizing interlayers [63, 169]. Some authors, however, attribute the increased ϵ_{CO} to deformation in the interlayer [176, 177], while other groups observe reduced ϵ_{CO} with the addition of a hardcoat and attribute this to reduced adhesion between film and substrate [178]. In any case, once cracks form in these brittle films, they propagate rapidly through the entire thickness of the coating and quickly extend large distances in a direction perpendicular to the applied strain [169]. At the substrate, the crack can also propagate along the coating/substrate interface (i.e. delamination), exacerbating the failure process [171, 179]. With additional strain, new cracks form and crack spacing decreases until a saturation spacing is reached [172, 173, 180], and with continued strain, transverse cracking and delamination of the fragments may also occur [63, 172, 173, 181]. In Fig. 3c, a strained ITO film on PET illustrates the microscopic appearance of several of these cracking and delamination phenomena.

The mismatching mechanical properties for compliant substrate/stiff electronics systems also creates considerable potential for device failure by delamination [184]. Under strain, mismatching properties (α , ν , E , etc.) lead to stresses that act directly on the interface, and if the interfacial toughness is low (i.e. poor adhesion), then debonding can occur. Generally, as interfacial stress increases, films will first slip a small distance with respect to the substrate ($\sim \mu\text{m}$), before beginning the process of complete delamination [182, 184]. It should also be noted that interfacial slipping or delamination are not necessarily restricted to the interface between the substrate and its immediate overlayer. Delamination or interfacial slip may occur at any interface in the device stack where the adhesion is poor, and cohesive failure, in which internal cracks in the plane of the film are responsible for debonding, has also been observed (e.g. for P3HT/PCBM photovoltaic devices) [185, 186].

Mechanics of bending-mode deformation

In a bending process, the two sides of a flexed sheet experience different types of strain. Tensile strain is present on the convex side, while the concave side experiences compressive strain. These strain states (shown in Fig. 4) may lead to different failure modes: components under tension tend to develop cracks, while components under compression (or with poor adhesion) tend to debond from the substrate [180, 187].

In a bent sheet, the greatest strains occur on the surfaces. In a homogeneous sheet, these peak strains can be approximated using the simple relation, $\epsilon_{\text{peak}} = t/2r$ [187, 188], or more accurate formulae that invoke fewer simplifying assumptions [168, 177, 189]. From these expressions, it is easy to note that thinner substrates experience lower peak strain at a given bending radius, and thus components mounted on these thinner substrates tend to tolerate smaller bending radii before failing. Moreover, through the bulk of a bent substrate, the strain varies between the compressive and tensile extremes on either surface. In a homogeneous film, the variation is linear, while in a layered structure the variation may be more complex, but in either case a “mechanically neutral plane” exists within the sheet where neither tensile nor compressive strain is present. Positioning fragile materials along this neutral plane (e.g. by patterning components on a substrate surface, then casting a mechanically equivalent thickness on top) maximizes the overall flexibility of the system. If the substrate and overlayer have similar mechanical properties, then equal thicknesses will ensure that the neutral plane lies at the position of the electronics. Or, if the substrate and overlayer are composed of mechanically distinct materials, then the electronics will lie in the neutral plane if

$$E_s t_s^2 = E_o t_o^2 \tag{8}$$

where E_s and t_s are the modulus and thickness of the substrate, and E_o and t_o are the modulus and thickness of the overlayer, respectively [168].

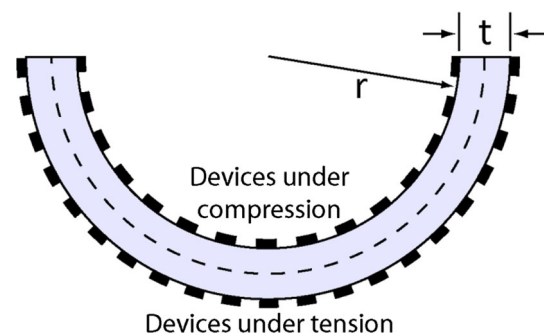


Fig. 4 Conceptual drawing of hypothetical electronic components (black rectangles) under compressive and tensile strain. The position of the mechanically neutral plane is also marked with a dashed line

A number of other analytical models have been developed to describe flexible devices under deformation. For example, Wu et al. modelled a three-layer system (consisting of a flexible substrate, an adhesive layer and an inorganic thin film) as elastic beams to determine how the properties of the adhesive could be varied to minimize the film strain during bending [190].

Mechanics of stretching-mode deformation

Because the neutral mechanical plane concept cannot be used to protect brittle components in a stretching-mode process, stretchability is generally considerably more difficult to engineer into an electronic system than bendability. Most methods of designing stretchability are implemented by avoiding straight paths in favour of meandering patterns wherever possible [5]. For electronic films restricted to the surface of a planar substrate, netlike [10, 191], meandering [112, 192–196], and even multi-level or fractal layouts [102, 197, 198] can be used to improve stretchability. These layouts always have longer electrical path lengths, but due to the influence of contact resistance, the overall increase in electrical resistance may not be substantial. Meandering conductors do, on the other hand, allow the pattern to twist or “unfold” with applied strain, thereby accommodating considerably greater strains than materials patterned along a straight line.

Another well-known method for engineering stretchability is through the formation of buckled morphologies that convert macroscopic stretching into local bending deformations. To implement the technique, compliant substrates are pre-strained in tension (in either 1D or 2D), then the electronic films are deposited and the pre-strain is released [89, 191, 199–206]. Because the films are generally stiffer than the substrates, they buckle out-of-plane during relaxation, forming corrugations while bonded to the substrate. In a pre-strain process, the buckling wavelength, λ , and amplitude, A , can be estimated by solving for the minimum elastic energy to find the relations:

$$\lambda = 2\pi t \left[\frac{E_f(1 - \nu_s^2)}{E_s(1 - \nu_f^2)} \right]^{1/3} \quad (9)$$

$$A = t \left[4\varepsilon_{\text{pre}} \left[\frac{E_f(1 - \nu_s^2)}{3E_s(1 - \nu_f^2)} \right]^{2/3} - 1 \right]^{1/2}, \quad (10)$$

where t is the film thickness, ε_{pre} is the pre-strain, E_f and E_s are the elastic moduli for film and substrate, and ν_f and ν_s are the Poisson's ratios for the film and substrate, respectively. The use of these simple equations is widespread, and some success in estimating the buckling geometry has been achieved. The simple equations are, however,

imperfect in that estimated λ and A values do not respond well to variations in pre-strain. Because of this, the equations have also been modified to more accurately account for the influence of pre-strain [100, 199, 205]:

$$\lambda = 2\pi t \left[\frac{E_f(1 - \nu_s^2)}{E_s(1 - \nu_f^2)} \right]^{1/3} \frac{1}{(1 + \varepsilon_{\text{pre}})(1 + \xi)^{1/3}} \quad (11)$$

$$A = t \left[4\varepsilon_{\text{pre}} \left[\frac{E_f(1 - \nu_s^2)}{3E_s(1 - \nu_f^2)} \right]^{2/3} - 1 \right]^{1/2} \frac{1}{(1 + \varepsilon_{\text{pre}})^{1/2}(1 + \xi)^{1/3}} \quad (12)$$

$$\xi = \frac{5\varepsilon_{\text{pre}}(1 + \varepsilon_{\text{pre}})}{32} \quad (13)$$

Provided that the electronic films remain undamaged throughout the buckling process [205], the materials are subsequently able to “unbuckle” to accommodate stretching-mode strain that is less than the original pre-strain. During unbuckling, the evolution of buckling wavelength and amplitude can be calculated based on the theory described by Jiang et al. [205].

Finite element analysis and materials models

Deriving analytical formulae that reliably describe mechanical behaviours becomes increasingly difficult as device complexity and strain increase. In order to predict the behaviour of more complex architectures, a numerical modelling technique known as finite element analysis (FEA) can often be employed [207]. Finite element analysis is a valuable tool for mapping field variables such as stress, strain and displacement that result when simulated forces or deformations (compression, bending, stretching, etc.) are applied to virtual models. In finite element analysis of a mechanical system, a body is discretized into a collection of pieces called “elements”, and analysis is performed at “nodes” (which lie at the intersections between elements). Solutions generally involve maps of parameters of interest over the discretized body [208]. The technique is extremely valuable both for exploring the influence of design parameters (such as geometry and material selections) over device behaviour and understanding the mechanisms of failure [178, 209].

Several software packages are utilized to implement FEA, including both commercial programs (ANSYS, Abaqus, etc.) and open-source freeware. In every case, the basic procedural steps are equivalent: pre-processing (which includes geometry construction, input of materials properties and discretization of the model), analysis (including tabulation and solution of relevant linear equations) and post-processing (display of solution). To perform an analysis, a physical system is first approximated

as a model with geometry defined either within the FEA software or by importing from a separate computer-aided design program. In many cases, geometric approximations are utilized to reduce computation time, such as solving a two-dimensional geometry when the system is not expected to vary in the third dimension.

The loading parameters and boundary conditions must also be described within the model. Boundary conditions may be expressed in terms of displacements (known as “essential boundary conditions”) or forces (known as “natural boundary conditions”). To match the reality of tensile testing experiments, uniform strain is defined at one end of a sample, while locking the displacement of the opposing edge to zero [210]. To mimic bending experiments, an out-of-plane displacement may be applied at one end, while displacement at the opposite end is fixed to zero.

Once the basic geometry is defined, the model is divided into discrete pieces during a process called “meshing”. Generally, the user manually defines an appropriate number of nodes/elements and chooses the element geometry. The FEA software then distributes these elements using an automated algorithm, ensuring that elements do not overlap and positioning nodes wherever the elements meet. An N -dimensional simulation (where N is the number of field variables evaluated at a given point) with M nodes requires $M \cdot N$ linear equations, and therefore choosing a reasonable mesh size is an important design problem. Simulations with more nodes/elements tend to more closely approximate the correct solution, but are also more computationally intensive (i.e. slower). Mesh size analysis should therefore typically be performed to determine the maximum mesh size for which the solution converges.

A plethora of element types are built into FEA software packages, and most packages also allow custom elements. Typical 2D mesh elements are triangular or quadrilateral in shape (where each corner corresponds to a node) [210], and 3D mesh elements are typically based on either solid elements (which connect along faces and may also be called brick elements) or shell elements (which connect along edges). A combination of elements may also be utilized; for example, Kim et al. used 4-node shell elements to model a thin film on a substrate represented as an 8-node brick element [211]. The values within an element may be interpolated from those at the nodes using an appropriate shape function for that particular element type.

Once the geometrical model is defined and meshed, the key to FEA is logically interrelating forces, F , and displacements, u , throughout the model to compile a set of solvable equations. Forces in one direction can lead to node displacements in any direction (cf., Poisson’s effect), so the set of equations relating forces and displacements take the general form:

$$F_i = \sum_j k_{ij} u_j, \quad (14)$$

where i and j each indicate combinations of both node and direction, F_i are nodal forces in i , u_j are displacements in j , and k_{ij} are the stiffness coefficients relating F_i and u_j . The fundamental theory that is used to define the stiffness coefficients, k_{ij} , is referred to as the “constitutive model” for the simulated material [212]. This model can be as simple as inputting the elastic modulus and Poisson’s ratio (i.e. a Hookean model); however, this is generally only valid for very small deformations. Elastomeric materials (such as PDMS) with moduli that vary as a function of strain are more suitably represented utilizing non-linear constitutive models, such as the Mooney–Rivlin hyperelastic model [212]. Metals are often modelled as plastically deformable solids using a power law, in which stress is related to strain by a hardening exponent, N , through the equation $\sigma = K\varepsilon^N$, where K is a prefactor [12]. Elastic–plastic models, in which different constitutive equations are applied below and above a defined transition point, may also be implemented for materials that are strained beyond their linear elastic range: for example, an elastic equation may be applied below the limit, and a power law above it [210]. Each material in the device stack can be expected to have a different array of material parameters, and therefore it is important to define an appropriate constitutive model for each and every material in a flexible device.

In most FEA of solids, the solution is found by minimizing the strain energy of the system: the set of equations describes the strain energy density at each node, and the optimum solution is the set of displacements (u_j) that minimizes the overall elastic energy [213]. From this solution, field variables such as stresses and strains can be calculated at the nodes, or with appropriate interpolation, throughout the elements. Results can be exported in tables or visualized in a variety of formats. While it is relatively straightforward to generate a model and evaluate a solution, demonstrating the validity of that model is more challenging. The modeller should evaluate scenarios with predictable outcomes and assess the logic of the generated solution, and models should be validated through comparison with experimental data whenever possible.

To predict failure through delamination, adhesion at the interface must be represented within the model. One approach is to utilize cohesive zone elements, treating delamination as a gradual separation of elements, and utilizing a traction separation law to relate the separation between nodes to a traction stress vector acting on those nodes. Within such a model, the traction separation vector increases to a critical value as the separation is increased, beyond this value the traction decreases, describing a

softening or (irreversible) degradation of the interface [210, 214, 215].

Mechanical characterization

Mechanical characterization techniques for flexible electronics applications can be sub-divided into two broad categories: (i) tests to determine mechanical constants and (ii) tests to track the evolution of device performance. The former group primarily involves the application of well-established mechanical characterization techniques, and data analysis is performed by more or less conventional means. Two well-known organizations, the American Society for Testing and Materials (ASTM) and the International Organization for Standardization (ISO), have developed thousands of standardized testing procedures for the repeatable characterization of a wide range of materials and systems. Existing standards are periodically updated and new standards are continuously added. Several standards are relevant to flexible electronic materials, and these are cited throughout this section [216–224].

Information about the performance of electronic devices under the influence of mechanical stresses or strains (i.e. the second category above) is extracted by several techniques, most of which involve measuring device performance metrics during mechanical deformation processes. In this review, we categorize these test procedures according to the mode of mechanical deformation, and we provide information in each category about the typical test equipment, device applications and the results obtained for the various classes of flexible electronic devices. Table 1 broadly summarizes this information by listing common test procedures and dominant failure modes under each type of deformation.

Determining materials constants

In order to describe a device in a finite element model or with an analytical equation, the basic material properties must first be known. A reasonable starting point is to utilize bulk values that are either reported in the literature or independently measured. These bulk properties are commonly measured using techniques such as tensile testing (in which samples are stretched in tension while recording stress and strain), dynamic mechanical analysis (in which a configurable sinusoidal force is applied to generate a sinusoidal stress–strain profile used to resolve the viscoelastic properties of the sample) or rheometry (for ultra-soft samples, gels, pastes and liquids). Each of these techniques can potentially be conducted over a range of temperatures, both to characterize materials at application-specific temperatures and also to determine glass transition

Table 1 Mechanical deformation modes and their effect on the materials/components in flexible electronics

Deformation mode (or testing mode)	Failure modes and test procedures
Bending	Delamination or slipping at hard/soft material interfaces [184] Cracking in functional coatings [165, 169, 171] Modulation in semiconductor charge carrier mobility [225, 226]
Stretching	Delamination and slipping at hard/soft material interfaces [184] Cracking in functional coatings [171, 227] Buckling of stiff functional materials on softer substrates [205, 228] ASTM standard: tensile properties of plastic sheeting [224]
Twisting	Buckling, delamination [229, 230] ASTM standard: torsion test [223]
Impact	ASTM standard: impact resistance of plastic sheeting [216]
Abrasion	Tensile cracking, substrate gouging [231, 232] ASTM standard: scratch resistance of plastics [222]
(Adhesion)	Tape test [217], peel test [233], scratch test [233], bend test [234]

temperatures, T_g , below which a material is rigid and glassy and above which a material is soft and rubbery.

The material properties for thin layers may, however, differ from bulk values, as differences in thickness can lead to microstructural variation [235]. Processing conditions also have a strong influence over film structure, such that different fabrication techniques may lead to materials with different mechanical properties [236]. Mechanically characterizing thin materials on a substrate is challenging, as the overall mechanical behaviour is derived from a combination of the properties of all the materials present. Nanoindentation is one technique that can be used to probe the properties of a thin film: this technique involves depressing a piezoelectrically controlled indenter tip into the surface of a material, while tracking the force/displacement curve [177, 237, 238]. Loading and unloading curves are collected, and provided that the shape of the indenter tip is well known, both the hardness and modulus may be calculated. The properties of the film can be adequately distinguished from the substrate when (1) the thickness of the film is at least ten times the indentation depth, and (2) the substrate is substantially stiffer than the film (to ensure that only the film deforms upon indentation) [239].

Another useful technique for determining the moduli of thin films on elastomeric substrates involves exploiting the buckling behaviour of the film [54–56, 58, 240, 241]. In

this method, a small compressive strain is applied to a film/substrate system (often by releasing a pre-strain maintained during film deposition), and this compression causes a rippled pattern to form. The spacing of these ripples (i.e. the buckling wavelength, λ) can be measured, and the film modulus can be calculated via reorganizing Eq. (9) to solve for E_f . This technique has been successfully applied to characterize a wide range of soft materials including functional materials for organic electronics with thicknesses from the nm to μm range [54, 241]. A “microtensile testing” technique has also been explored for measuring the elastic moduli of small-scale sub-micron thin films [242].

Bending deformation

To characterize the bending-mode strain tolerance of flexible electronics, the evolution of device performance metrics is measured during a mechanical bending process. Several variables can be used to describe the deformation magnitude, and the most common of these is the radius of curvature (or bending radius), r , to which the sample is subjected (smaller r corresponds to a larger deformation). Because substrate thickness also influences strain in a bending process (see above), many authors perform the very useful geometry-based calculations to relate bending radius to the actual strain that is imparted to the electronic materials. With these calculations, the device’s performance parameters can be plotted against mechanical strain, which allows the strain tolerance of the electronics to be assessed (rather than strain tolerance of the electronics/substrate system) and enables convenient comparisons across publications. Reporting device performance against bending strain is the norm in most cases. Other sporadically reported variables include curvature, which is the inverse of bending radius, and “bending angle”, which is the angle formed between the two ends of a bent sample. Bending angle, however, is not easily compared across publications as it tends to be specific to each apparatus and sample configuration.

Bending the sample toward the electronics imparts compressive strain, while bending the sample away from the electronics imparts tensile strain, and in each case three classes of experiments are typically performed: (i) simple before/after measurements in which a single bending process is performed, (ii) cyclic measurements in which performance is assessed during many successive strain cycles or (iii) variable strain experiments in which device performance is evaluated against bending radius or strain.

In the most basic experiment, a researcher first measures the as-fabricated device performance according to established procedures, then bends the device by hand and remeasures its performance. This procedure provides some limited information about the resilience of the device. To

apply quantified bending, samples are often manually wrapped around rods of known diameter (Fig. 5a), but this approach still suffers from several drawbacks, including unpredictable abrasion during wrapping and unintentional variations in the strain cycle due to the manual sample handling. The former issue often precludes compressive strains from being applied because devices come into direct contact with the rod, and even in cases where only tensile deformation is imposed, the potential still exists for film damage to occur during handling. This additional damage is especially problematic if it occurs unpredictably and the researcher fails to identify the variation in test conditions. It is also important to note that manually applying a strain cycle that deforms every region of the sample uniformly and reproducibly is difficult, if not impossible; variations in strain rate (i.e. wrapping speed), mechanical forces (in all directions) and ambient conditions can all influence the degradation of a device, so ideally these parameters should all be measured, controlled and reported.

The best experimental designs entirely decouple the experiment from human interaction by automating the test procedure, with the ideal measurement apparatus, (i) imposing uniform bending strain over an entire sample, (ii) applying controlled bending strains, strain rates and forces,

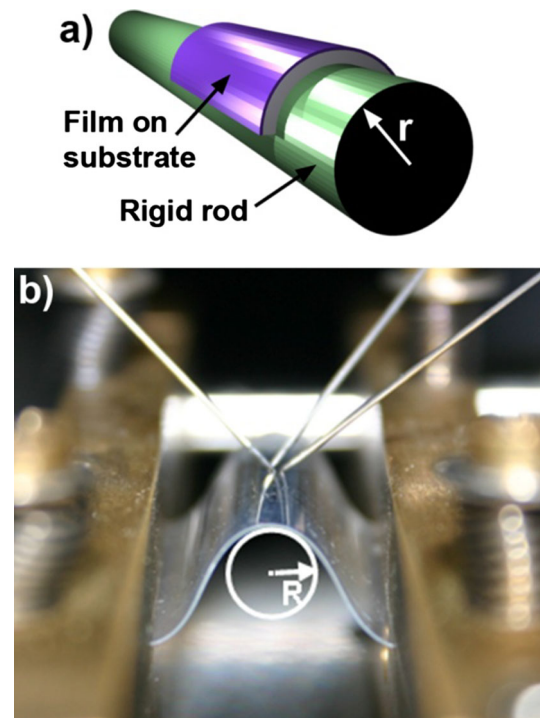


Fig. 5 **a** Illustration of bending strain applied by wrapping samples around a rigid rod. Reproduced with permission from [243]. **b** Photograph of a bending apparatus incorporating a linear translation stage. The designers of this particular device highlight the non-uniform sample curvature and carefully probe the sample at the apex of the bend ($R = 2.5$ mm). Reproduced with permission from [244]

(iii) minimizing contact with the sample and (iv) automatically measuring and calculating all relevant device performance parameters in situ. It is difficult to design equipment with all of these in mind, but several devices certainly deliver more reliable data than manual wrapping experiments. One of the most common mechanized approaches is to affix the two ends of a substrate to plates on a translation stage [187]. An image illustrating this scheme is shown in Fig. 5b, and from the image it can be inferred that greater bending strains are applied as the plates are brought closer together. This approach is advantageous because the experimenter does not necessarily handle the sample during testing, but care must still be taken to ensure that the strain cycles are reproducible. It must also be understood that with this apparatus, bending strain is not uniform over the entire sample, and the maximum strain is only applied at the apex of the bend. To address this, some apparatuses implement an arc-like (rather than linear) motion [245], while others roll samples around a mandrel of known diameter [227].

Abrasion-induced degradation at electrical contacts also represents a considerable problem, and it is very likely that many efforts to address this practical issue are not reported. Minimizing motion at all points of contact is the best approach, but metallic lubricants, such as eGaIn, have also been added at the contacts to reduce abrasion by the electrical probes [226].

Bending-mode tests to evaluate the strain tolerance of flexible electronics are widespread in the literature, and plots of device-specific performance metrics during bending deformations have been published for most materials and devices. These include, for instance, insulators and barrier layers [246, 247], electrical conductors [152, 248–254] and transparent conductors. When discussing transparent conductors, common themes include tracking the mechanical degradation of the brittle transparent conducting oxides (especially ITO) [64, 227, 255–261] or developing more strain-tolerant alternatives [28, 243, 256, 261–281]. Numerous transparent conductors that outperform ITO from a strain tolerance standpoint have now been described, although it is interesting that few comparisons of bending-induced failure among the different classes of non-TCO materials have appeared to date. In addition to electrical conductivity, transparent conductors must also exhibit light transmission, yet measurements of bending-mode strain tolerance usually neglect optical properties. Light transmission and transparent conductor figures-of-merit during strain cycling are generally not discussed, and this is likely due to the difficulty in aligning optical components within a mechanical bending apparatus and synchronizing light transmission measurements with the strain cycle.

Another class of devices that is highly relevant for flexible electronics is thin-film transistors, and numerous

bending-mode deformation studies have now been completed for these devices [73, 189, 225, 226, 244, 282–297]. One common observation is charge carrier mobility that decreases as devices are bent in one direction (i.e. tension/compression), but increases when bent in the opposite. The direction of response, however, is not consistent across all semiconductor/dielectric pairs, and the effect has been attributed to strain-induced variations in the electron orbitals at the interface [226]. Sekitani et al. perform extensive mechanical testing on pentacene-based FETs positioned in a neutral mechanical plane, including cyclic testing to 160,000 bending cycles [225], and in a separate publication [283], the minimum bending radii that various TFT materials systems endure before failure are catalogued. These authors (and others) [292] also note that the direction of strain with respect to the semiconducting channel plays a role in determining strain tolerance.

Bending-mode deformation studies have also been completed on flexible solar cells [243, 298–300]; however, incident light power profiles tend to complicate the investigation of bending-mode strain tolerance. The spatial power distribution for most solar simulators is calibrated to uniformly deliver 100 mW/cm² at a fixed measurement plane. As samples are bent out of this fixed plane, the spatial and/or spectral power distribution may depart somewhat from that of the typical measurement plane. Moreover, the solid angle for light absorption, waveguiding and reflected power all vary with the light incidence angle, and these effects collectively lead to some uncertainty in the measured performance metrics for solar cells. To address this issue, researchers may accept the uncertainty [298, 299], return the device to the flattened state before conducting the solar cell evaluation [243] or perform cyclic testing at various radii [299].

Experiments to track the evolution of device performance parameters during bending have also been published for passive capacitors and inductors [301], supercapacitor systems [302–306], energy scavengers [2, 307, 308], batteries [309–319], light-emitting devices [264, 320–327], memory devices [328–345], touch screens/pressure sensors [346–349], antennas [350, 351], waveguides [352] and other electronic circuits [200, 283, 295, 353]. Overall, bending is an extremely important deformation mode that must be fully characterized to facilitate the development of reliable flexible electronic devices. Both the characteristics of individual components and integrated systems must be considered.

Stretching deformation

In a stretching-mode measurement, the performance parameters for the electronic device under test are continuously or periodically recorded during tensile strain processes, and three basic types of measurements are common:

(i) simple before/after measurements, (ii) linearly increasing strain or (iii) cyclic stretching to a fixed maximum strain. The strain axis may or may not be important, depending upon the layout of the particular device, but in any case the device performance can be recorded as the sample is uniaxially, biaxially or otherwise stretched along any axis or axes that are practical. Commercial testing equipment that can apply well-controlled stresses and strains to clamped samples at prescribed strain rates is widely available (see, for example, the apparatus in Fig. 6), and therefore it is relatively rare to read descriptions of manually imposed stretching of electronic devices published in the literature. The test equipment generally records force and displacement data, and from these data the stress–strain curves can be generated using Eqs. (1) and (3). The most relevant ASTM standards deal with tensile tests of plastic sheeting [224]. Sample geometry is a key factor, and in most published plots a simplification is made: both stress and strain are calculated based on the initial sample geometry, rather than the dynamically evolving geometry (i.e. $A = A_0$, and the presence of non-uniformities is neglected). These simplified parameters are formally

called “engineering stress” and “engineering strain”, but usually the adjectives are dropped. Some publications, on the other hand, account for the evolving sample geometry, and the corrected values are referred to as “true stress” and “true strain” [162].

In stretching experiments, clamping is an extremely important issue, and steps must be taken to ensure that the sample is contacted firmly enough to prevent slipping while also avoiding any abrasive damage. For highly deformable samples such as elastomers, over-tightening the clamps must also be avoided to prevent excessive sample compression and unintended damage near the clamps. To prevent scratches, relative motion between the sample and clamps should be avoided as much as possible (this is especially problematic during loading), and similarly any points of contact with external equipment (including electrical probes, detectors, lenses, etc.) should be designed to minimize relative motion. When making contact with external equipment, it is also important to restrict the stretching motion as little as possible. For example, stiff electrical contacts positioned at actively deforming locations (i.e. between the tensile tester clamps) can modify the stress/strain conditions in their vicinity. More accurate test results may be generated using sliding contacts (provided abrasion is not an issue) or positioning the contacts at stationary locations (e.g. outside the clamps).

Another complicating factor, in this case pertaining to data analysis, is the often complex variation in sample geometry that occurs during stretching. For example, in a uniaxial strain process, samples elongate, but they also become narrower and thinner simultaneously. These transverse contractions (depicted in the inset of Fig. 6) are described by Poisson’s ratio, but it is important to understand that this ratio does not necessarily remain constant throughout an entire strain process, particularly if large strains extending beyond the elastic limit are imposed. If the mechanical environment is not uniform, the “Poisson’s ratios” may also be quite different for sample width contractions versus thickness contractions. A conducting film and its mechanically distinct substrate, for instance, are forced to deform as a unit along the width direction, but are free of this restriction in the thickness direction. Therefore, it is not always safe to assume that Poisson’s ratios measured under any particular set of conditions are static and valid for other experimental scenarios.

Near the clamps, another strain-dynamic geometry issue can complicate analysis: the sample width is pinned at the clamps, so the width (and thickness) tends to taper between the clamp and the sample bulk. The length and shape of the taper (also shown in the inset of Fig. 6) vary with strain, and the properties of the materials or devices within the taper must certainly be assumed to differ from those throughout the rest of the sample. If any of the active

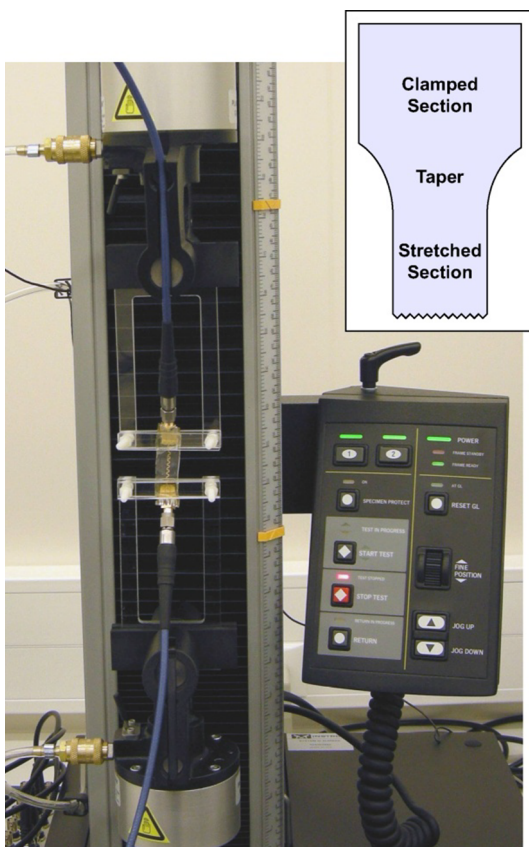


Fig. 6 Typical apparatus for a stretching-mode strain experiment. As a sample is stretched, it becomes thinner and narrower, while also developing a pronounced taper near the clamps. Reproduced with permission from [193]

components are located within this tapered region, data analysis could become considerably more complicated than expected, and therefore it is best to keep all active materials far from the clamps wherever possible. If this cannot be avoided (such as for analysis of films or devices that extend through the clamps), then the sample length should be as large as is practical to reduce the influence of this tapered region.

If the sample is mechanically inhomogeneous (even if by design), then it is quite possible that behaviour under strain could be even more unpredictable. For example, a material comprising distinct stiff and compliant sections will preferentially deform in the most compliant regions. In this case, *in situ* microscopy or finite element models may be necessary to truly understand the geometry over the entire sample. All of these geometry issues highlight the importance of rationally considering the evolution of sample geometry and understanding how it influences the analysis. In some cases, geometric variations will be largely irrelevant. This could include evaluation of “complete” electronic circuits by tracking a particular electrical signal during strain. If the important parameters are entirely independent of geometry, then it may not be necessary to understand that geometry in great detail. On the other hand, if geometric parameters are used anywhere in the analysis (e.g. in the calculations of power conversion efficiency in a solar cell, charge carrier mobility in a transistor or resistivity in an electrical conductor), then it may be critically important to directly track the dimensions of the sample or devices throughout the stretching experiment and use only these measured dimensions for all calculations.

A host of flexible electronic materials and devices have been evaluated in stretching-mode experiments. Extensive tests of strain tolerance have, for example, been performed on electrical conductors [15, 16, 71, 72, 123, 152, 192–194, 197, 248–251, 320, 354–363]. Among these publications, Graz et al. performed an extended study of homogeneous gold thin films under cyclic strain [362], and extensive studies of conductors patterned in a strain-tolerant meandering patterns were performed by Bossuyt et al. and Hsu et al. [192, 194]. Stretching-mode strain tolerance has also been evaluated for a wide range of transparent conductors [163, 173, 227, 243, 262, 269, 305, 346, 364–367]. Most studies tend to report the increase in raw electrical resistance with strain, although some include geometrical analysis and report the evolution of sheet resistance or resistivity [163, 359, 366]. The most complete strain tolerance studies tend to focus on ITO [173, 227, 368], and the degradation of this material under uniaxial strain is becoming well understood. In recent publications, however, a common theme is the development of new transparent conductors with strain tolerance considerably

superior to ITO. This has certainly been accomplished, although few side-by-side comparisons among the more strain-tolerant materials have yet been published [367]. Most studies also note that electrical degradation of transparent conductors is more problematic than optical degradation and do not address the variation in light transmission that occurs during strain. Against this trend, one publication demonstrates improved transmission for a stretched Au nanomesh [269], and two others report the evolution of transparent conductor sheet resistance, transmission and figure-of-merit [366, 369].

Several examples of complete stretchable electronic devices tested under uniaxial strain have also been reported in the literature. These include published plots of device-specific performance parameters for stretchable solar cells [55, 240, 370–373], thin-film transistors [73, 285, 360, 374–378], diodes [202, 375], capacitors [81, 123, 354, 365], supercapacitors [304, 305, 379–385], batteries [102, 386–390], mechanical energy harvesters [391], light-emitting devices [3, 249, 359, 361, 392], antennas [17, 18, 197, 393–399], electronic circuits [4, 112, 200, 211, 400] and biomedical devices [109]. Kaltenbrunner et al. [370] performed uniaxial, biaxial and cyclic stretching strain tolerance studies for P3HT:PCBM solar cells fabricated on extremely thin plastic substrates, and Lipomi et al. [240] published an excellent mechanical study showcasing solar cells formed using strain-tolerant electrodes and two different photoactive compositions. In each publication, photovoltaic performance metrics were recorded during various strain processes, and the authors focussed their discussion on mechanisms leading toward strain tolerance. For TFTs, some of the trends noted in bending mode have been reproduced in stretching experiments. This includes carrier mobility that linearly increases/decreases with strain and partially recovers with relaxation [285]. Gaikwad et al. [386] published current/voltage characteristics, impedance/frequency maps and electrical discharge curves for stretchable batteries under several strain conditions, and Liang et al. [392] showed plots of current density, luminance and efficiency versus tensile strain up to 120 % for stretchable OLEDs on polyurethane acrylate substrates. Kubo et al. [18] characterized RF antennas under stretching-mode strain by reporting reflected power and resonant frequency for both linearly increasing and cyclic tensile strains up to 120 %, and Kim et al. [200] formed stretchable ring oscillator and differential amplifier circuitry and recorded the variation in voltage outputs under various strain conditions.

Variations in device performance as a function of deformation have further been exploited to engineer strain sensors that can withstand much larger deformations than traditional inorganic devices [10, 17, 115, 123, 126, 153, 354, 365, 393, 396, 401]. These flexible strain and pressure

sensors are of particular interest for biomedical applications, and therefore the devices must remain functional over the large range of deformations which skin and other tissues regularly exhibit.

Shear/twisting deformation

Flexible electronic devices deployed into everyday use are also certain to be subjected to shear, which is a stress/strain state that occurs when parallel planes within a sample are forced in opposing directions. Bending can be considered a shear strain, and a range of other simple motions such as twisting, tearing or rubbing also generate shear [402]. For example, the shear force exerted on a surface by a fingertip during tactile perception has been estimated to be ~ 8 N [403, 404], and therefore reliable electronic devices must withstand shear forces much greater than this. While shear is often ignored, it is as critical as any other mechanical deformation mode.

Several common tests of shear properties impose stresses and strains using a twisting motion known as torsion [223], and the progression of a torsion experiment (shown in Fig. 7a) is tracked by continuously recording the twist angle, θ , and applied torque, T . Few descriptions of mechanical tests of flexible electronics in shear/torsion have appeared in the literature. Torsion tests of electrical conductors [251], microfluidic antennas [395], LED arrays [3] and complex flexible circuits including inverters, ring oscillators and amplifiers [211] have been performed, and the mechanics of twisting/shear deformations were specifically studied (including calculations of the maximum locally induced strains) for interconnects bonded at each end to a substrate [203, 405]. Adhesive electrical interconnects designed for mounting rigid ICs to flexible substrates have also been assessed in shear [229], but the electronics themselves were not designed to deform in these experiments. The shear resistance of electrically conducting threads adhered to the contact pads of textile-integrated temperature sensors has been studied in shear using a force gauge, and the shear resistance of these components was found to be on par with that of flip-chipped IC devices [404]. LCDs have also been tested both under progressively increasing shear strain and strain cycling at 2 Hz to a maximum of 20,000 cycles [406, 407]. A simple twisting-mode experiment was also performed on a stretchable battery, by demonstrating that the device could power an LED while twisted 90° [386].

Adhesion, cohesion and scratch testing

Good adhesion between all the materials in a device stack is vital in the formation of useful flexible electronic devices because external loading can provide the energy to separate

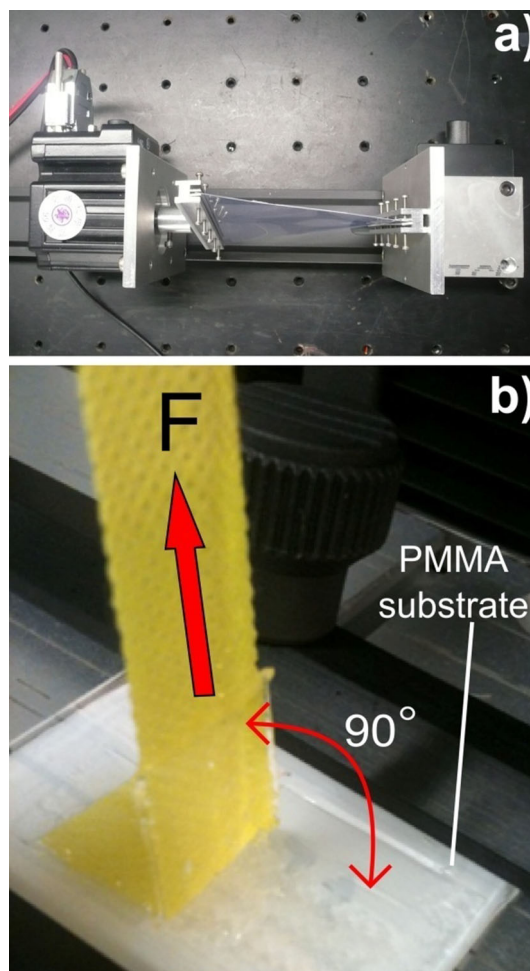


Fig. 7 **a** Photograph of a torsion testing apparatus. Reproduced with permission from [402]. **b** Photograph of a materials system set up for peel testing. In this case, the adhesion of a PDMS/PMMA interface is being probed by embedding a polyester fabric directly within the PDMS overlayer and applying force to the fabric. Reproduced with permission from [408]

poorly bonded materials from one another and render the device inoperable. In most practical experiments, adhesion is quantified by reporting the force or energy required to separate the constituent materials. Flexible devices could be evaluated in this manner, with the energy required to disrupt the weakest interface determining the functional adhesive strength of the device. In the case of strong adhesion between layers, the constituent materials may also individually fail before failure occurs at an interface (i.e. cohesive rather than adhesive failure).

Numerous methods for evaluating adhesion strength between two layers have been developed, and some excellent reviews of these techniques are available [233, 234, 409]. One extremely simple qualitative test, known as the “tape test” [217, 233], involves merely affixing and removing an adhesive tape. In conventional tape tests, optical inspection

is used to determine if the film remains intact following the test, but for functional electronics, before/after or cyclic measurements of device-specific performance parameters can also be recorded. These simple tape tests have been performed on various flexible conductors [250, 253, 254, 320], transparent conductors [26, 261, 265, 268, 270, 410–412], fuel cell membranes [412] and batteries [413]. These tape tests are useful, yet they are also highly qualitative: no numerical values for adhesion are obtained, the tests results cannot generally be compared from publication-to-publication (or even from experimenter-to-experimenter), and the tests are limited to investigating adhesive strengths less than that between the tape and film (which could itself vary with the type of tape utilized).

Other, more quantitative tests are available, and these have been used to determine thin-film adhesion for a variety of materials. Peel testing is a mechanized variation of the tape test used to quantify adhesive forces [233, 234]. In this test, the adhesive tape (or even the film itself) is attached to a motor and load cell, and a mechanical force is applied while the opposing material is held firmly in place. As the two materials of interest are separated, force/displacement data are recorded. In Fig. 7b, a peel test is shown with a tensile tester physically pulling on a piece of fabric (yellow colour) embedded in a PDMS film; strong adhesion between the fabric and the film is critical for achieving quantitative measurements. Most of the disadvantages inherent to manual tape tests (noted above) remain in place, but quantitative data can be collected [414]. Several substrates with surface treatments intended to improve adhesion of electronic materials have been assessed in peel tests [415], as have transparent conductors [416], and complete organic solar cells [417, 418]. The results of peel tests have also been used to inform stretchable electronics numerical modelling studies [183]. A “dual cantilever beam” mode has also been used to reveal adhesion information [416–418]. In this mode, a test sample is firmly affixed (with an appropriate adhesive) between two plates, and these plates are then separated while recording force/displacement data. The test structure is forced to fail somewhere within the device stack, and the force/displacement curve can be analysed to determine failure energy. This technique has been employed to measure adhesion/cohesion properties of several solar cell architectures [416–418].

Scratch testing methods [218, 221, 222, 231–234] have also been used to assess the interfacial strength of electronic materials. In these tests, a stylus is forced into contact with the sample and translated across the surface, inducing shear stress at the substrate/film interface. This interface will fail if shear forces exceed a critical load correlated with the interfacial strength, so in the most useful scratch tests, the load is linearly increased during the test in order to determine this critical load. The technique

has been criticized (primarily due to difficulties in accurately identifying when failure occurs, and also in establishing reliable comparisons when different styluses or substrates are utilized) [233], but it does remain a well-established technique for evaluating adhesion. Several examples of application to flexible electronics have been published including evaluation of critical loads for several transparent conductors [238, 346, 419–421], piezoelectric transducers [420] and both semiconductors and dielectrics for FETs [414, 415].

Observation and analysis of bending processes [185, 186, 234, 422, 423] has also been used to measure the adhesion/cohesion of material sets intended for flexible electronics. Generally, samples are deformed (often using a four-point bend geometry) while collecting force/displacement data, and post-analysis reveals parameters such as critical loads for adhesive/cohesive failure and adhesive/cohesive energy. Vibration [420], indentation [234, 238] and pulsed laser irradiation [181] have also been used to induce failure in analyses of adhesive/cohesive strength.

Impact resistance

In the hands of consumers, flexible electronics are also quite certain to be shock loaded as products are dropped, struck with objects or subjected to weathering (e.g. hail). A product's ability to withstand these loading conditions is assessed in tests of “impact resistance”, and several ASTM standards are available that describe the equipment used in these tests [216, 219, 220]. Generally, impact experiments are performed by releasing an object of known geometry above a test specimen and delivering a calculable quantity of kinetic energy to the sample. In an impact experiment with full support, the sample is placed on a rigid plate with no relief structures, while in an impact experiment with partial support, the test specimen is only supported at few points and the load is applied at a position between the supports. In either case, the supports should be designed to ensure that they do not deform during the experiment and that the kinetic load is dissipated exclusively within the sample itself. Once the load impacts the test specimen, the kinetic energy can either be absorbed elastically or inelastically. Energy absorbed elastically typically recovers, leading to “bouncing” of the load, while inelastic absorption leads to permanent damage of the test specimen. The outcome of the experiment is usually quantified by reporting “mean failure energy”, where “failure” is defined as the creation of any visible damage on the test specimen. These experiments could conceivably be adapted to flexible electronics simply by redefining “failure” as a change in any device-specific performance parameter by a pre-defined amount.

Descriptions of impact tests as applied to flexible electronics are limited. The adhesive interconnects between

rigid ICs and flexible substrates were assessed in drop tests [424], and the contact resistance was found to increase roughly linearly with absorbed impact energy, while the slope increased with humidification. Complete LCDs have also been evaluated in ball drop impact tests [406], and it was found that fully supported devices tended to fail with modest ball drop heights (~ 4 cm), while partially supported devices flexed to absorb considerable impact energy and recovered without suffering damage.

Techniques to improve the durability of flexible systems

In the sections above, techniques to characterize a variety of systems—from individual components to integrated devices—have been described. The ultimate purpose is to improve the operation of these devices under a variety of mechanical conditions. As illustrated in the typical deformable device shown in Fig. 8, the development of complete flexible electronics systems necessitates a combination of several diverse materials within a single platform. Because stress concentrations may become severe at the hard/soft interfaces, the junctions between materials are typically the source of device failure during deformation [188]. This problem has long been recognized as a major challenge for reliable operation, and in the following subsections techniques that have been used to mitigate the problem are reviewed.

Engineering stress distribution across layers

When exposed to frequent bending or stretching, cracks develop in the stiffest materials, and layers with mismatching mechanical properties may debond. To solve this, early

studies concentrated on the failure mechanics of alternating organic/inorganic layers [63, 174, 425]. These studies guided the development of optimal flexible encapsulation layers for organic light-emitting diodes (OLEDs), where extremely limited oxygen/water permeation ($\sim 10^{-6}$ g/m²/day) is required to achieve a reasonable lifetime ($>10,000$ h) [179, 187]. Utilizing this fundamental understanding of failure mechanics in layered heterogeneous structures, Suo et al. [168] suggested positioning the most brittle components in a neutral mechanical plane, as described above. Positioning the brittle components (usually semiconductors and oxides; often active devices) at the neutral plane and surrounding them with more strain-tolerant layers (usually the substrate and encapsulation layers) creates a more mechanically robust system. This simple concept has been employed as one of the most basic principles for array-level integration of flexible electronics [200, 288, 299].

Nanoribbons and nanomembranes

Nanomembranes are freestanding materials, where thickness is less than a few hundred nanometers [426], and nanoribbons include only the subset of these nanomembranes where one lateral dimension is orders of magnitude shorter than the other. Each of these nanostructures can be used to dramatically improve a material's bendability. Semiconductor nanomembranes and nanoribbons, for example, are well known for photon/phonon confinement effects and unusual optical/thermoelectrical behaviour [427]. In the bulk, inorganic semiconductor materials have large moduli (~ 150 GPa for Si, ~ 85 GPa for GaAs) and undergo brittle fracture at strains of $\sim 1\%$ or less [198]. With aggressive thinning, however, 200-nm-thick free-standing nanoribbons clearly show considerable flexibility (Fig. 9a). This behaviour is due to the fact that bending

Fig. 8 Simplified anatomy of a flexible electronics system. In general, hard and soft materials can typically be found in electronically active and passive components, respectively. The interfaces between mechanically dissimilar materials are prone to failure during mechanical stress cycles

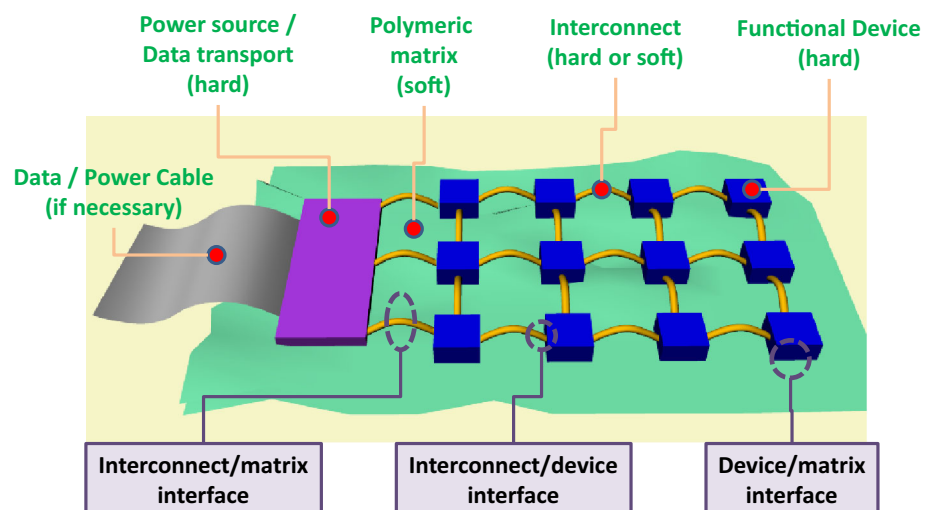
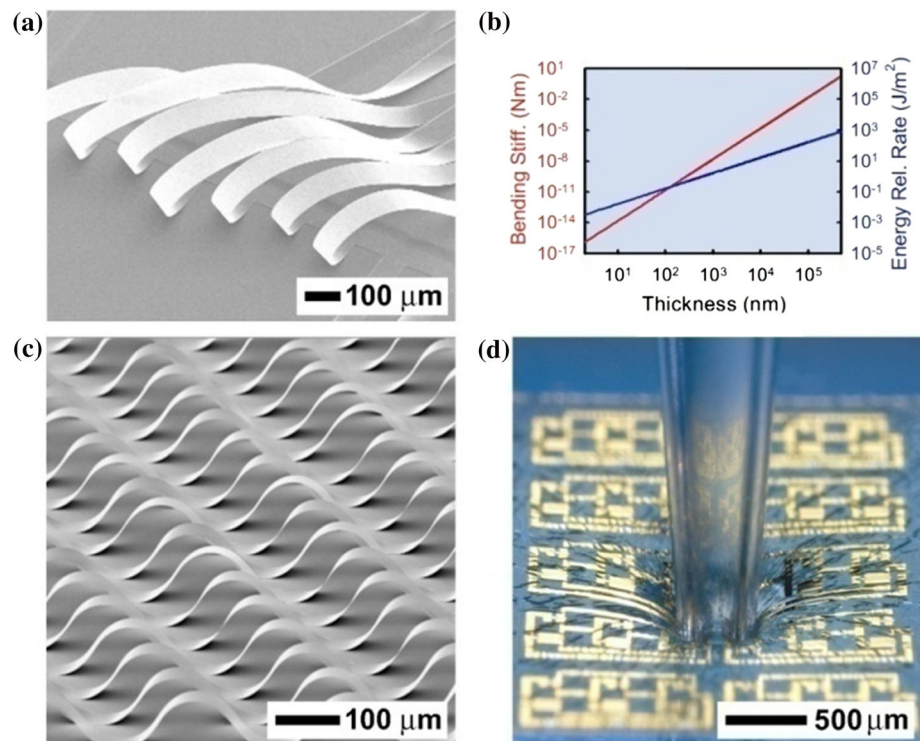


Fig. 9 **a** SEM image of an array of released silicon nanoribbons with a thickness of ~ 300 nm. **b** The bending stiffness of silicon membranes (red) and energy release rate for thermally driven delamination (blue) as a function of the membrane thickness between 2 nm and $200\ \mu\text{m}$. The plot indicates that 2-nm-thick nanomembranes have $\sim 10^{15}$ times less flexural rigidity and are $\sim 10^5$ times more adherent to the substrate than $200\text{-}\mu\text{m}$ -thick counterparts. **c** SEM image of a wavy array of GaAs nanoribbons on a PDMS substrate. **d** Optical image of stretchable CMOS circuit with single-crystalline silicon nanoribbons. Reproduced with permission from (a) [198], (b) [426], (c) [202] and (d) [431] (Color figure online)



stiffness and bending-induced strains scale with the cubic and linear power of thickness (Fig. 9b). In a dramatic example that rigid materials are rendered flexible when dimensions are reduced into the nano-regime, nanomembranes of brittle semiconductors (such as GaAs) were rolled into nanotubes under the action of residual stress [428–430]. With this approach, two or more layers of semiconductors are grown epitaxially, and upon release from the substrate, differences in the interatomic distances cause compressive (tensile) stress on the layer with larger (smaller) lattice parameter. This lattice mismatch then leads to a bending strain that rolls the bilayer structures into nanotubes with diameter down to a half micron [428].

To fabricate nanomembranes or nanoribbons in practise, controlled delamination is often employed [89, 170, 191, 199, 203, 432]. In a homogeneous film/substrate system with poor adhesion, compressive strain can induce spontaneous delamination, leading to “delamination blisters” with a spatial periodicity characteristic of the mechanical properties of the film/substrate system. By relaxing pre-strain (as described above), these delamination blisters can be induced controllably, thereby rendering the system stretchable. The technique is further refined by pre-patterning the substrate for selective adhesion. Localized UV/ozone treatment of PDMS, for example, leads to selective adhesion of Si or GaAs nanoribbons, and invoking the pre-strain relaxation procedure on such a patterned substrate leads to controlled delamination at untreated areas [202]. With this process, the

designer is able to pre-select advantageous film/substrate bonding sites (at connections with circuit elements, for example) and utilize the remainder of the material to introduce strain tolerance. Rogers et al., for example, harvested single-crystalline semiconductor nanoribbons from silicon-on-insulator [375] and GaAs [202] wafers, and transfer printed onto pre-strained PDMS substrates. When the pre-strain was relaxed, the nanoribbons formed periodic, wavy structures on the elastomeric substrate (Fig. 9c) with wavelengths defined by lithographically patterned bonding. The wavy structure naturally provides stretchability (up to $\sim 100\%$), compressibility (up to $\sim 25\%$) and bendability (with radius of curvature down to 5 mm) for GaAs nanoribbons [202]. It is important to note, however, that out-of-plane devices and interconnects may be especially vulnerable to abrasion or scratching. For device reliability, it may be necessary to situate these out-of-plane components in protected cavities or otherwise encapsulate them [371].

Single-crystalline inorganic semiconductor nanoribbons formed through controlled delamination have enabled a wide range of array-level integrated flexible/stretchable electronics (Fig. 9d) [200, 433]. It is also notable that nanotubes possess extreme bendability and have been utilized in system-level integration of flexible/stretchable electronics [50, 287, 433, 434]. Graphene and other 2D materials are also promising options to maximize the merits of nanomembranes and nanoribbons by reducing the layer thickness into the atomic level [262, 435, 436].

Separation of brittle components

Spatial separation of brittle components is perhaps the most influential strategy for array integration of stretchable electronics. The basic idea is rather simple: instead of tightly grouping the brittle components, they are dispersed across the substrate. Regions between the brittle components are then optimized for strain tolerance (by, for example, utilizing interconnects formed with controlled delamination, as discussed above), which alleviates the danger of stress localization at the brittle components. Given that semiconductors (such as silicon, III–V materials or pentacene) tend to be the materials most susceptible to strain-induced damage, this lateral separation concept has been applied to form flexible ICs with laterally spaced semiconductor devices interconnected with stretchable conductors (Fig. 10) [14, 201, 211, 437]. In these circuits, the logic/switching elements are well separated from one another, and power sources/communication modules (which are generally stiff and use a sizable area fraction) are also broken into discrete pieces and distributed across the substrate. Development was a heavily collaborative effort, and the history and significance are archived in a handful of review papers [14, 89, 108, 198, 438].

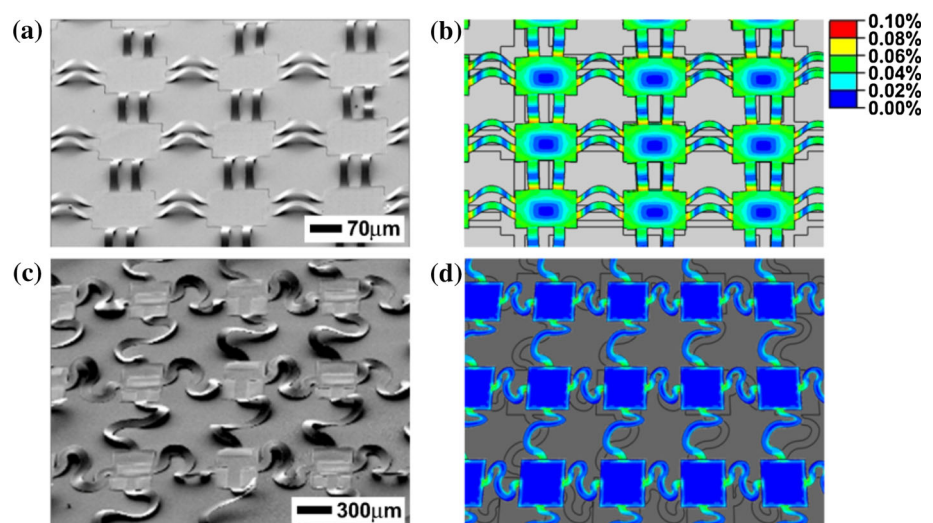
An advanced approach involves local modification of the substrate to mechanically reinforce regions where brittle components are intended to be positioned. Early efforts from Wagner's group at Princeton resulted in stiff inorganic islands interconnected by compliant metallic conductors patterned on a soft substrate [195, 439], and the concept was further enhanced by tuning the local stiffness of a PDMS substrate by controlling the cross-linking density [72, 374]. In this latter work, the key lies in patterning a photoinhibitor within the PDMS. These elementary technologies led to system-level integration, where

macroscopic ICs (mm to cm scale) were directly embedded in an elastomer matrix to allow immediate commercialization [193, 440, 441]. The greatest merit of this approach is that chip reliability under severe operating conditions has already been established, and thus only the resilience of the interconnects requires verification [358]. The downside is, of course, compromised flexibility (due to the rigid and bulky ICs) and the possibility of delamination.

Summary and outlook

The field of flexible electronics is rich and diverse, with a wide assortment of useful devices currently under intense development. Most of these emerging devices have rigid analogues, such that the introduction of flexibility is intended to broaden the range of applications where the devices may be implemented. Consider a solar cell, for example: rigid modules are excellent energy harvesters, but flexible variants might be integrated into clothing or manufactured in a roll, then cut to length on request. Other emerging devices, such as many implantable biomedical interfaces, simply could not be realized without the ongoing advances of flexible electronics research. In any review of the field, the reader must certainly be armed with an understanding of these various classes of flexible devices, and therefore we began by discussing basic technologies, operating mechanisms, performance metrics and the key research challenges involved in the development of these devices. This overview immediately draws attention to the central role played by device mechanics in the overall reliability of a flexible electronic system, and therefore an introduction to device mechanics as written for the non-expert was included. This discussion involved crack formation/evolution, factors driving interfacial delamination

Fig. 10 SEM images (*left*) and mechanical models (*right*, strain colour scale shown on far right) of two different interconnect structures with controlled buckling for high-performance stretchable electronics. In **a** and **b**, silicon nanomembranes are selectively bonded at the nodes of a mesh, and arc-shaped interconnects bridge the electronically active nodes. In **c** and **d**, the interconnects have non-coplanar meandering shapes with improved strain tolerance. Reproduced with permission from **a**, **b** and **d** [108], and **c** [211]



and mechanics principles specific to bending and stretching deformations of brittle films on compliant substrates. The various means of evaluating strain tolerance of electronic devices (grouped according to deformation type, i.e. bending, stretching, twisting, delamination, scratching and impact) were then discussed in detail, and throughout this section, we included information intended to guide the reader in designing the most effective and trustworthy measurements of strain tolerance. Finally, we discussed advanced concepts for pre-designed strain tolerance in flexible devices: positioning fragile components along neutral planes, engineering controlled out-of-plane deformations, and distributing the most brittle components over a large, selectively reinforced area.

Looking forward, it is exceedingly clear that opportunity still remains to enhance the mechanical resilience of flexible electronic devices. One emerging concept that is worth highlighting is that of “molecularly stretchable electronics”, i.e. materials designed for innate stretchability by virtue of their molecular structures rather than geometry [39]. Through controlled copolymerization of electronically active monomers, it may be possible to form mechanically compliant forms of most components of flexible electronics. This approach potentially eliminates the source of mechanical failure on a fundamental level, although challenges may come in ensuring that the electronic properties are adequate.

A rather interesting approach for interconnecting cm-scale chips was recently suggested by the Rogers group [4]. Here, all the electrical components are first fully encapsulated followed by immersion in silicone oil (i.e. an uncrosslinked viscous monomer) to mitigate abrasion that may occur during operation. The silicone oil and devices are then hermetically packaged within stretchable elastomers. This concept does, however, increase the volume of system and carries some danger that oil may leak if the packaging is punctured.

Finally, it is worth mentioning that the future of flexible electronics may advance beyond the concept of stretchable macroelectronics. For example, the Lieber group at Harvard suggested a new concept employing 3D networks of nanowire sensors embedded in a tissue scaffold [442]. Hydrogels that are extremely tough and resilient can revolutionize the field of stretchable electronics [443], where most of the substrate materials are currently silicone or polyurethane based. Invasive electronic networks and hydrogels are important motifs that can lead to artificial tissues, bioimplants and robotics applications. With this diversification of materials and device form factors, mechanical testing and fundamental understanding of device mechanics will be increasingly important for the future of the field.

Compliance with ethical standards

Conflict of interest The authors declare that they have no conflict of interest.

References

- Mannsfeld SCB, Tee BCK, Stoltenberg RM, Chen CVHH, Barman S, Muir BVO, Sokolov AN, Reese C, Bao ZN (2010) Highly sensitive flexible pressure sensors with microstructured rubber dielectric layers. *Nat Mater* 9:859–864
- Dagdeviren C, Yang BD, Su YW, Tran PL, Joe P, Anderson E, Xia J, Doraiswamy V, Dehdashti B, Feng X, Lu BW, Poston R, Khalpey Z, Ghaffari R, Huang YG, Slepian MJ, Rogers JA (2014) Conformal piezoelectric energy harvesting and storage from motions of the heart, lung, and diaphragm. *Proc Natl Acad Sci* 111:1927–1932
- Kim RH, Kim DH, Xiao JL, Kim BH, Park SI, Panilaitis B, Ghaffari R, Yao JM, Li M, Liu ZJ, Malyarchuk V, Kim DG, Le AP, Nuzzo RG, Kaplan DL, Omenetto FG, Huang YG, Kang Z, Rogers JA (2010) Waterproof AllnGaP optoelectronics on stretchable substrates with applications in biomedicine and robotics. *Nat Mater* 9:929–937
- Xu S, Zhang YH, Jia L, Mathewson KE, Jang KI, Kim J, Fu HR, Huang X, Chava P, Wang RH, Bhole S, Wang LZ, Na YJ, Guan Y, Flavin M, Han ZS, Huang YG, Rogers JA (2014) Soft microfluidic assemblies of sensors, circuits, and radios for the skin. *Science* 344:70–74
- Cheng T, Zhang Y, Lai W-Y, Huang W (2015) Stretchable thin-film electrodes for flexible electronics with high deformability and stretchability. *Adv Mater* 27:3349–3376
- Park S, Vosguerichian M, Bao ZA (2013) A review of fabrication and applications of carbon nanotube film-based flexible electronics. *Nanoscale* 5:1727–1752
- Perelaer J, Smith PJ, Mager D, Soltman D, Volkman SK, Subramanian V, Korvink JG, Schubert US (2010) Printed electronics: the challenges involved in printing devices, interconnects, and contacts based on inorganic materials. *J Mater Chem* 20:8446–8453
- Huang D, Liao F, Molesa S, Redinger D, Subramanian V (2003) Plastic-compatible low resistance printable gold nanoparticle conductors for flexible electronics. *J Electrochem Soc* 150:G412–G417
- Lipomi DJ, Bao ZA (2011) Stretchable, elastic materials and devices for solar energy conversion. *Energy Environ Sci* 4:3314–3328
- Sekitani T, Someya T (2010) Stretchable, large-area organic electronics. *Adv Mater* 22:2228–2246
- Benight SJ, Wang C, Tok JBH, Bao ZA (2013) Stretchable and self-healing polymers and devices for electronic skin. *Prog Polym Sci* 38:1961–1977
- Xiang Y, Li T, Suo ZG, Vlassak JJ (2005) High ductility of a metal film adherent on a polymer substrate. *Appl Phys Lett* 87:161910
- Li T, Suo Z (2006) Deformability of thin metal films on elastomer substrates. *Int J Solids Struct* 43:2351–2363
- Wagner S, Bauer S (2012) Materials for stretchable electronics. *MRS Bull* 37:207–217
- Zhu S, So JH, Mays R, Desai S, Barnes WR, Pourdeyhimi B, Dickey MD (2013) Ultrastretchable fibers with metallic conductivity using a liquid metal alloy core. *Adv Funct Mater* 23:2308–2314

16. Park J, Wang SD, Li M, Ahn C, Hyun JK, Kim DS, Kim DK, Rogers JA, Huang YG, Jeon S (2012) Three-dimensional nanonetworks for giant stretchability in dielectrics and conductors. *Nat Commun* 3:916
17. Cheng S, Wu ZG (2011) A microfluidic, reversibly stretchable, large-area wireless strain sensor. *Adv Funct Mater* 21:2282–2290
18. Kubo M, Li XF, Kim C, Hashimoto M, Wiley BJ, Ham D, Whitesides GM (2010) Stretchable microfluidic radiofrequency antennas. *Adv Mater* 22:2749–2752
19. Cheng S, Wu ZG (2012) Microfluidic electronics. *Lab Chip* 12:2782–2791
20. Baca AJ, Ahn JH, Sun YG, Meitl MA, Menard E, Kim HS, Choi WM, Kim DH, Huang Y, Rogers JA (2008) Semiconductor wires and ribbons for high-performance flexible electronics. *Angew Chem Int Ed* 47:5524–5542
21. Long YZ, Yu M, Sun B, Gu CZ, Fan ZY (2012) Recent advances in large-scale assembly of semiconducting inorganic nanowires and nanofibers for electronics, sensors and photovoltaics. *Chem Soc Rev* 41:4560–4580
22. Liu X, Long YZ, Liao L, Duan XF, Fan ZY (2012) Large-scale integration of semiconductor nanowires for high-performance flexible electronics. *ACS Nano* 6:1888–1900
23. Wu JH, Zang JF, Rathmell AR, Zhao XH, Wiley BJ (2013) Reversible sliding in networks of nanowires. *Nano Lett* 13:2381–2386
24. Sun DM, Liu C, Ren WC, Cheng HM (2013) A review of carbon nanotube- and graphene-based flexible thin-film transistors. *Small* 9:1188–1205
25. Hecht DS, Hu LB, Irvin G (2011) Emerging transparent electrodes based on thin films of carbon nanotubes, graphene, and metallic nanostructures. *Adv Mater* 23:1482–1513
26. Hu LB, Kim HS, Lee JY, Peumans P, Cui Y (2010) Scalable coating and properties of transparent, flexible, silver nanowire electrodes. *ACS Nano* 4:2955–2963
27. Lee JY, Connor ST, Cui Y, Peumans P (2008) Solution-processed metal nanowire mesh transparent electrodes. *Nano Lett* 8:689–692
28. Rathmell AR, Bergin SM, Hua YL, Li ZY, Wiley BJ (2010) The growth mechanism of copper nanowires and their properties in flexible, transparent conducting films. *Adv Mater* 22:3558–3563
29. Yao SS, Zhu Y (2015) Nanomaterial-enabled stretchable conductors: strategies, materials and devices. *Adv Mater* 27:1480–1511
30. Huang JC (2002) Carbon black filled conducting polymers and polymer blends. *Adv Polym Technol* 21:299–313
31. Strumpler R, Glatz-Reichenbach J (1999) Conducting polymer composites. *J Electroceram* 3:329–346
32. Zhang W, Dehghani-Sani AA, Blackburn RS (2007) Carbon based conductive polymer composites. *J Mater Sci* 42:3408–3418. doi:10.1007/s10853-007-1688-5
33. Nyholm L, Nystrom G, Mihranyan A, Stromme M (2011) Toward flexible polymer and paper-based energy storage devices. *Adv Mater* 23:3751–3769
34. Snook GA, Kao P, Best AS (2011) Conducting-polymer-based supercapacitor devices and electrodes. *J Power Sources* 196:1–12
35. Bhadra S, Khastgir D, Singha NK, Lee JH (2009) Progress in preparation, processing and applications of polyaniline. *Prog Polym Sci* 34:783–810
36. Halpin JC (1969) Stiffness and expansion estimates for oriented short fiber composites. *J Compos Mater* 3:732–734
37. Rafiee MA, Rafiee J, Wang Z, Song HH, Yu ZZ, Koratkar N (2009) Enhanced mechanical properties of nanocomposites at low graphene content. *ACS Nano* 3:3884–3890
38. Horowitz G (2006) Organic transistors. In: Klauk H (ed) *Organic electronics, materials, manufacturing and applications*. Wiley-VCH, Weinheim, pp 3–32
39. Savagatrup S, Printz AD, O'Connor TF, Zaretski AV, Lipomi DJ (2014) Molecularly stretchable electronics. *Chem Mater* 26:3028–3041
40. Heeger AJ (2001) Nobel lecture: semiconducting and metallic polymers: the fourth generation of polymeric materials. *Rev Mod Phys* 73:681–700
41. Elschner A, Kirchmeyer S, Lovenich W, Merker U, Reuter K (2011) PEDOT: principles and applications of an intrinsically conductive polymer. CRC Press, New York
42. Weiss NO, Zhou HL, Liao L, Liu Y, Jiang S, Huang Y, Duan XF (2012) Graphene: an emerging electronic material. *Adv Mater* 24:5782–5825
43. Lee C, Wei XD, Kysar JW, Hone J (2008) Measurement of the elastic properties and intrinsic strength of monolayer graphene. *Science* 321:385–388
44. Kang J, Shin D, Bae S, Hong BH (2012) Graphene transfer: key for applications. *Nanoscale* 4:5527–5537
45. Torrisi F, Hasan T, Wu WP, Sun ZP, Lombardo A, Kulmala TS, Hsieh GW, Jung SJ, Bonaccorso F, Paul PJ, Chu DP, Ferrari AC (2012) Inkjet-printed graphene electronics. *ACS Nano* 6:2992–3006
46. Sun YG, Rogers JA (2007) Inorganic semiconductors for flexible electronics. *Adv Mater* 19:1897–1916
47. Guillen C, Herrero J (2011) TCO/metal/TCO structures for energy and flexible electronics. *Thin Solid Films* 520:1–17
48. Hecht DS, Kaner RB (2011) Solution-processed transparent electrodes. *MRS Bull* 36:749–755
49. Layani M, Kamyshny A, Magdassi S (2014) Transparent conductors composed of nanomaterials. *Nanoscale* 6:5581–5591
50. Lu W, Lieber CM (2006) Semiconductor nanowires. *J Phys D Appl Phys* 39:R387–R406
51. Katz HE, Huang J (2009) Thin-film organic electronic devices. *Annu Rev Mater Res* 39:71–92
52. Wang XS, Tang HP, Li XD, Hua X (2009) Investigations on the mechanical properties of conducting polymer coating-substrate structures and their influencing factors. *Int J Mol Sci* 10:5257–5284
53. Biswas C, Lee YH (2011) Graphene versus carbon nanotubes in electronic devices. *Adv Funct Mater* 21:3806–3826
54. Tahk D, Lee HH, Khang DY (2009) Elastic moduli of organic electronic materials by the buckling method. *Macromolecules* 42:7079–7083
55. Savagatrup S, Makaram AS, Burke DJ, Lipomi DJ (2014) Mechanical properties of conjugated polymers and polymer-fullerene composites as a function of molecular structure. *Adv Funct Mater* 24:1169–1181
56. O'Connor B, Chan EP, Chan C, Conrad BR, Richter LJ, Kline RJ, Heeney M, McCulloch I, Soles CL, DeLongchamp DM (2010) Correlations between mechanical and electrical properties of polythiophenes. *ACS Nano* 4:7538–7544
57. Awartani O, Lemanski BI, Ro HW, Richter LJ, DeLongchamp DM, O'Connor BT (2013) Correlating stiffness, ductility, and morphology of polymer:fullerene films for solar cell applications. *Adv Energy Mater* 3:399–406
58. Savagatrup S, Printz AD, Rodriguez D, Lipomi DJ (2014) Best of both worlds: conjugated polymers exhibiting good photovoltaic behavior and high tensile elasticity. *Macromolecules* 47:1981–1992
59. Printz AD, Savagatrup S, Burke DJ, Purdy TN, Lipomi DJ (2014) Increased elasticity of a low-bandgap conjugated copolymer by random segmentation for mechanically robust solar cells. *RSC Adv* 4:13635–13643

60. Green MA, Ho-Baillie A, Snaith HJ (2014) The emergence of perovskite solar cells. *Nat Photonics* 8:506–514
61. Snaith HJ (2013) Perovskites: the emergence of a new era for low-cost, high-efficiency solar cells. *J Phys Chem Lett* 4:3623–3630
62. Cao Q, Xia MG, Shim M, Rogers JA (2006) Bilayer organic-inorganic gate dielectrics for high-performance, low-voltage, single-walled carbon nanotube thin-film transistors, complementary logic gates, and p-n diodes on plastic substrates. *Adv Funct Mater* 16:2355–2362
63. Leterrier Y (2003) Durability of nanosized oxygen-barrier coatings on polymers—internal stresses. *Prog Mater Sci* 48:1–55
64. Zardetto V, Brown TM, Reale A, Di Carlo A (2011) Substrates for flexible electronics: a practical investigation on the electrical, film flexibility, optical, temperature, and solvent resistance properties. *J Polym Sci B Polym Phys* 49:638–648
65. Fortunato G, Pecora A, Maiolo L (2012) Polysilicon thin-film transistors on polymer substrates. *Mater Sci Semicond Process* 15:627–641
66. Nathan A, Ahnood A, Cole MT, Lee S, Suzuki Y, Hiralal P, Bonaccorso F, Hasan T, Garcia-Gancedo L, Dyadyusha A, Haque S, Andrew P, Hofmann S, Moultrie J, Chu DP, Flewitt AJ, Ferrari AC, Kelly MJ, Robertson J, Amaratunga GAJ, Milne WI (2012) Flexible electronics: the next ubiquitous platform. *Proc IEEE* 100:1486–1517
67. Xu Y (2013) Post-CMOS and post-MEMS compatible flexible skin technologies: a review. *IEEE Sens J* 13:3962–3975
68. Toivola M, Halme J, Miettunen K, Aitola K, Lund PD (2009) Nanostructured dye solar cells on flexible substrates. *Int J Energy Res* 33:1145–1160
69. MacDonald WA, Looney MK, MacKerron D, Eveson R, Rakos K (2008) Designing and manufacturing substrates for flexible electronics. *Plast Rubber Compos* 37:41–45
70. MacDonald WA, Looney MK, MacKerron D, Eveson R, Adam R, Hashimoto K, Rakos K (2007) Latest advances in substrates for flexible electronics. *J Soc Inf Disp* 15:1075–1083
71. Vijay V, Rao AD, Narayan KS (2011) In situ studies of strain dependent transport properties of conducting polymers on elastomeric substrates. *J Appl Phys* 109:084525
72. Cotton DPI, Popel A, Graz IM, Lacour SP (2011) Photopatterning the mechanical properties of polydimethylsiloxane films. *J Appl Phys* 109:054905
73. Takahashi T, Takei K, Gillies AG, Fearing RS, Javey A (2011) Carbon nanotube active-matrix backplanes for conformal electronics and sensors. *Nano Lett* 11:5408–5413
74. Tobjork D, Osterbacka R (2011) Paper electronics. *Adv Mater* 23:1935–1961
75. Hu LB, Cui Y (2012) Energy and environmental nanotechnology in conductive paper and textiles. *Energy Environ Sci* 5:6423–6435
76. Lukowicz P, Kirstein T, Troster G (2004) Wearable systems for health care applications. *Methods Inf Med* 43:232–238
77. Park S, Jayaraman S (2003) Smart textiles: wearable electronic systems. *MRS Bull* 28:585–591
78. Salvado R, Loss C, Goncalves R, Pinho P (2012) Textile materials for the design of wearable antennas: a survey. *Sensors* 12:15841–15857
79. Axisa F, Schmitt PM, Gehin C, Delhomme G, McAdams E, Dittmar A (2005) Flexible technologies and smart clothing for citizen medicine, home healthcare, and disease prevention. *IEEE Trans Inf Technol Biomed* 9:325–336
80. Zeng W, Shu L, Li Q, Chen S, Wang F, Tao XM (2014) Fiber-based wearable electronics: a review of materials, fabrication, devices, and applications. *Adv Mater* 26:5310–5336
81. Hu LB, Pasta M, La Mantia F, Cui LF, Jeong S, Deshazer HD, Choi JW, Han SM, Cui Y (2010) Stretchable, porous, and conductive energy textiles. *Nano Lett* 10:708–714
82. Sazonov A, Meitine M, Stryakhilev D, Nathan A (2006) Low-temperature materials and thin-film transistors for electronics on flexible substrates. *Semiconductors* 40:959–967
83. Zhang K, Seo JH, Zhou WD, Ma ZQ (2012) Fast flexible electronics using transferrable silicon nanomembranes. *J Phys D Appl Phys* 45:143001
84. Cho JH, Lee J, Xia Y, Kim B, He YY, Renn MJ, Lodge TP, Frisbie CD (2008) Printable ion-gel gate dielectrics for low-voltage polymer thin-film transistors on plastic. *Nat Mater* 7:900–906
85. Zaumseil J, Sirringhaus H (2007) Electron and ambipolar transport in organic field-effect transistors. *Chem Rev* 107:1296–1323
86. Chung HJ, Kim TI, Kim HS, Wells SA, Jo S, Ahmed N, Jung YH, Won SM, Bower CA, Rogers JA (2011) Fabrication of releasable single-crystal silicon-metal oxide field-effect devices and their deterministic assembly on foreign substrates. *Adv Funct Mater* 21:3029–3036
87. Kim TI, Jung YH, Chung HJ, Yu KJ, Ahmed N, Corcoran CJ, Park JS, Jin SH, Rogers JA (2013) Deterministic assembly of releasable single crystal silicon-metal oxide field-effect devices formed from bulk wafers. *Appl Phys Lett* 102:182104
88. Han ST, Zhou Y, Roy VAL (2013) Towards the development of flexible non-volatile memories. *Adv Mater* 25:5425–5449
89. Kim DH, Xiao JL, Song JZ, Huang YG, Rogers JA (2010) Stretchable, curvilinear electronics based on inorganic materials. *Adv Mater* 22:2108–2124
90. Kim TI, Kim RH, Rogers JA (2012) Microscale inorganic light-emitting diodes on flexible and stretchable substrates. *IEEE Photon J* 4:607–612
91. Tok JBH, Bao ZA (2012) Recent advances in flexible and stretchable electronics, sensors and power sources. *Sci China Chem* 55:718–725
92. Weerasinghe HC, Huang FZ, Cheng YB (2013) Fabrication of flexible dye sensitized solar cells on plastic substrates. *Nano Energy* 2:174–189
93. Dennler G, Sariciftci NS (2005) Flexible conjugated polymer-based plastic solar cells: from basics to applications. *Proc IEEE* 93:1429–1439
94. Angmo D, Krebs FC (2013) Flexible ITO-free polymer solar cells. *J Appl Polym Sci* 129:1–14
95. Xie KY, Wei BQ (2014) Materials and structures for stretchable energy storage and conversion devices. *Adv Mater* 26:3592–3617
96. Goetzberger A, Hebling C, Schock HW (2003) Photovoltaic materials, history, status and outlook. *Mater Sci Eng, R* 40:1–46
97. Lee SY, Choi KH, Choi WS, Kwon YH, Jung HR, Shin HC, Kim JY (2013) Progress in flexible energy storage and conversion systems, with a focus on cable-type lithium-ion batteries. *Energy Environ Sci* 6:2414–2423
98. Gwon H, Hong J, Kim H, Seo DH, Jeon S, Kang K (2014) Recent progress on flexible lithium rechargeable batteries. *Energy Environ Sci* 7:538–551
99. Zhou GM, Li F, Cheng HM (2014) Progress in flexible lithium batteries and future prospects. *Energy Environ Sci* 7:1307–1338
100. Zhang Y, Huang Y, Rogers JA (2015) Mechanics of stretchable batteries and supercapacitors. *Curr Opin Solid State Mater Sci* 19:190–199
101. Bates JB, Dudney NJ, Neudecker B, Ueda A, Evans CD (2000) Thin-film lithium and lithium-ion batteries. *Solid State Ionics* 135:33–45

102. Xu S, Zhang YH, Cho J, Lee J, Huang X, Jia L, Fan JA, Su YW, Su J, Zhang HG, Cheng HY, Lu BW, Yu CJ, Chuang C, Kim TI, Song T, Shigeta K, Kang S, Dageviren C, Petrov I, Braun PV, Huang YG, Paik U, Rogers JA (2013) Stretchable batteries with self-similar serpentine interconnects and integrated wireless recharging systems. *Nat Commun* 4:1543
103. Koo JH, Seo J, Lee T (2012) Nanomaterials on flexible substrates to explore innovative functions: from energy harvesting to bio-integrated electronics. *Thin Solid Films* 524:1–19
104. Chen Y, Lu BW, Ou DP, Feng X (2015) Mechanics of flexible and stretchable piezoelectrics for energy harvesting. *Sci China Phys Mech Astron* 58:594601
105. Roberts ME, Sokolov AN, Bao ZN (2009) Material and device considerations for organic thin-film transistor sensors. *J Mater Chem* 19:3351–3363
106. Hammock ML, Chortos A, Tee BCK, Tok JBH, Bao ZA (2013) The evolution of electronic skin (e-skin): a brief history, design considerations, and recent progress. *Adv Mater* 25:5997–6037
107. Kim DH, Ghaffari R, Lu NS, Rogers JA (2012) Flexible and stretchable electronics for biointegrated devices. *Annu Rev Biomed Eng* 14:113–128
108. Kim DH, Lu NS, Huang YG, Rogers JA (2012) Materials for stretchable electronics in bioinspired and biointegrated devices. *MRS Bull* 37:226–235
109. Minev IR, Musienko P, Hirsch A, Barraud Q, Wenger N, Moraud EM, Gandar J, Capogrosso M, Milekovic T, Asboth L, Torres RF, Vachicouras N, Liu Q, Pavlova N, Duis S, Larmagnac A, Voros J, Micera S, Suo Z, Courtine G, Lacour SP (2015) Electronic dura mater for long-term multimodal neural interfaces. *Science* 347:159–163
110. Rivnay J, Owens RM, Malliaras GG (2014) The rise of organic bioelectronics. *Chem Mater* 26:679–685
111. Jeong J-W, Shin G, Park SI, Yu KJ, Xu L, Rogers JA (2015) Soft materials in neuroengineering for hard problems in neuroscience. *Neuron* 86:175–186
112. Kim DH, Lu NS, Ma R, Kim YS, Kim RH, Wang SD, Wu J, Won SM, Tao H, Islam A, Yu KJ, Kim TI, Chowdhury R, Ying M, Xu LZ, Li M, Chung HJ, Keum H, McCormick M, Liu P, Zhang YW, Omenetto FG, Huang YG, Coleman T, Rogers JA (2011) Epidermal electronics. *Science* 333:838–843
113. Yeo WH, Kim YS, Lee J, Ameen A, Shi LK, Li M, Wang SD, Ma R, Jin SH, Kang Z, Huang YG, Rogers JA (2013) Multifunctional epidermal electronics printed directly onto the skin. *Adv Mater* 25:2773–2778
114. Jang KI, Han SY, Xu S, Mathewson KE, Zhang YH, Jeong JW, Kim GT, Webb C, Lee JW, Dawidczyk TJ, Kim RH, Song YM, Yeo WH, Kim S, Cheng HY, Il Rhee S, Chung J, Kim B, Chung HU, Lee DJ, Yang YY, Cho M, Gaspar JG, Carbonari R, Fabiani M, Gratton G, Huang YG, Rogers JA (2014) Rugged and breathable forms of stretchable electronics with adherent composite substrates for transcutaneous monitoring. *Nat Commun* 5:4779
115. Huang X, Liu YH, Cheng HY, Shin WJ, Fan JA, Liu ZJ, Lu CJ, Kong GW, Chen K, Patnaik D, Lee SH, Hage-Ali S, Huang YG, Rogers JA (2014) Materials and designs for wireless epidermal sensors of hydration and strain. *Adv Funct Mater* 24:3846–3854
116. Bandodkar AJ, Jia WZ, Wang J (2015) Tattoo-based wearable electrochemical devices: a review. *Electroanalysis* 27:562–572
117. Bandodkar AJ, Hung VWS, Jia WZ, Valdes-Ramirez G, Windmiller JR, Martinez AG, Ramirez J, Chan G, Kerman K, Wang J (2013) Tattoo-based potentiometric ion-selective sensors for epidermal pH monitoring. *Analyst* 138:123–128
118. Bandodkar AJ, Molinnus D, Mirza O, Guinovart T, Windmiller JR, Valdes-Ramirez G, Andrade FJ, Schoning MJ, Wang J (2014) Epidermal tattoo potentiometric sodium sensors with wireless signal transduction for continuous non-invasive sweat monitoring. *Biosens Bioelectron* 54:603–609
119. Kim J, de Araujo WR, Samek IA, Bandodkar AJ, Jia WZ, Brunetti B, Paixao TRLC, Wang J (2015) Wearable temporary tattoo sensor for real-time trace metal monitoring in human sweat. *Electrochem Commun* 51:41–45
120. Windmiller JR, Bandodkar AJ, Valdes-Ramirez G, Parkhomovsky S, Martinez AG, Wang J (2012) Electrochemical sensing based on printable temporary transfer tattoos. *Chem Commun* 48:6794–6796
121. Bandodkar AJ, Nuñez-Flores R, Jia W, Wang J (2015) All-printed stretchable electrochemical devices. *Adv Mater* 27:3060–3065
122. Lumelsky VJ, Shur MS, Wagner S (2001) Sensitive skin. *IEEE Sens J* 1:41–51
123. Lipomi DJ, Vosgueritchian M, Tee BCK, Hellstrom SL, Lee JA, Fox CH, Bao ZN (2011) Skin-like pressure and strain sensors based on transparent elastic films of carbon nanotubes. *Nat Nanotechnol* 6:788–792
124. Wagner S, Lacour SP, Jones J, Hsu PHI, Sturm JC, Li T, Suo ZG (2004) Electronic skin: architecture and components. *Physica E* 25:326–334
125. Chortos A, Bao Z (2014) Skin-inspired electronic devices. *Mater Today* 17:321–331
126. Kim J, Lee M, Shim HJ, Ghaffari R, Cho HR, Son D, Jung YH, Soh M, Choi C, Jung S, Chu K, Jeon D, Lee S-T, Kim JH, Choi SH, Hyeon T, Kim D-H (2014) Stretchable silicon nanoribbon electronics for skin prostheses. *Nat Commun* 5:5747
127. Viventi J, Kim DH, Vigeland L, Frechette ES, Blanco JA, Kim YS, Avrin AE, Tiruvadi VR, Hwang SW, Vanleer AC, Wulsin DF, Davis K, Gelber CE, Palmer L, Van der Spiegel J, Wu J, Xiao JL, Huang YG, Contreras D, Rogers JA, Litt B (2011) Flexible, foldable, actively multiplexed, high-density electrode array for mapping brain activity in vivo. *Nat Neurosci* 14:1599–1605
128. Khaled I, Elmallah S, Cheng C, Moussa WA, Mushahwar VK, Elias AL (2013) A flexible base electrode array for intraspinal microstimulation. *IEEE Trans Biomed Eng* 60:2904–2913
129. Zrenner E, Bartz-Schmidt KU, Benav H, Besch D, Bruckmann A, Gabel VP, Gekeler F, Greppmaier U, Harscher A, Kibbel S, Koch J, Kusnyerik A, Peters T, Stingl K, Sachs H, Stett A, Szurman P, Wilhelm B, Wilke R (2011) Subretinal electronic chips allow blind patients to read letters and combine them to words. *Proc R Soc B* 278:1489–1497
130. Xu LZ, Gutbrod SR, Bonifas AP, Su YW, Sulkin MS, Lu NS, Chung HJ, Jang KI, Liu ZJ, Ying M, Lu C, Webb RC, Kim JS, Laughner JI, Cheng HY, Liu YH, Ameen A, Jeong JW, Kim GT, Huang YG, Efimov IR, Rogers JA (2014) 3D multifunctional integumentary membranes for spatiotemporal cardiac measurements and stimulation across the entire epicardium. *Nat Commun* 5:3329
131. Potter-Baker KA, Capadona JR (2015) Reducing the “stress”: antioxidative therapeutic and material approaches may prevent intracortical microelectrode failure. *ACS Macro Lett* 4:275–279
132. Holt DJ, Grainger DW (2012) Host response to biomaterials. In: Hollinger JO (ed) *An introduction to biomaterials*. Taylor & Francis Group, Boca Raton, FL, pp 91–118
133. Marin C, Fernandez E (2010) Biocompatibility of intracortical microelectrodes: current status and future prospects. *Front Neuroeng* 3:1–6
134. Prasad A, Sanchez JC (2012) Quantifying long-term microelectrode array functionality using chronic in vivo impedance testing. *J Neural Eng* 9:026028
135. Biran R, Martin DC, Tresco PA (2005) Neuronal cell loss accompanies the brain tissue response to chronically implanted silicon microelectrode arrays. *Exp Neurol* 195:115–126

136. Campbell SA (2001) The science and engineering of micro-electronic fabrication. Oxford University Press, Oxford, UK
137. Alf ME, Asatekin A, Barr MC, Baxamusa SH, Chelawat H, Ozaydin-Ince G, Petruczuk CD, Sreenivasan R, Tenhaeff WE, Trujillo NJ, Vaddiraju S, Xu JJ, Gleason KK (2010) Chemical vapor deposition of conformal, functional, and responsive polymer films. *Adv Mater* 22:1993–2027
138. Kim H, Lee HBR, Maeng WJ (2009) Applications of atomic layer deposition to nanofabrication and emerging nanodevices. *Thin Solid Films* 517:2563–2580
139. Knez M, Niesch K, Niinisto L (2007) Synthesis and surface engineering of complex nanostructures by atomic layer deposition. *Adv Mater* 19:3425–3438
140. Moonen PF, Yakimets I, Huskens J (2012) Fabrication of transistors on flexible substrates: from mass-printing to high-resolution alternative lithography strategies. *Adv Mater* 24:5526–5541
141. Krebs FC (2009) Polymer solar cell modules prepared using roll-to-roll methods: knife-over-edge coating, slot-die coating and screen printing. *Sol Energy Mater Sol Cells* 93:465–475
142. Krebs FC, Gevorgyan SA, Alstrup J (2009) A roll-to-roll process to flexible polymer solar cells: model studies, manufacture and operational stability studies. *J Mater Chem* 19:5442–5451
143. Jain K, Klosner M, Zemel M, Raghunandan S (2005) Flexible electronics and displays: high-resolution, roll-to-roll, projection lithography and photoablation processing technologies for high-throughput production. *Proc IEEE* 93:1500–1510
144. Treutlein R, Bergsmann M, Stonley CJ (2006) Reel-to-reel vacuum metallization. In: Klauk H (ed) *Organic electronics, materials, manufacturing and applications*. Wiley-VCH, Weinheim, pp 183–202
145. Reinhold E, Faber J (2011) Large area electron beam physical vapor deposition (EB-PVD) and plasma activated electron beam (EB) evaporation—Status and prospects. *Surf Coat Technol* 206:1653–1659
146. Ludwig R, Kukla R, Josephson E (2005) Vacuum web coating—state of the art and potential for electronics. *Proc IEEE* 93:1483–1490
147. Juang ZY, Wu CY, Lu AY, Su CY, Leou KC, Chen FR, Tsai CH (2010) Graphene synthesis by chemical vapor deposition and transfer by a roll-to-roll process. *Carbon* 48:3169–3174
148. Kukla R, Ludwig R, Meinel J (1996) Overview on modern vacuum web coating technology. *Surf Coat Technol* 86–7:753–761
149. Kessels WMM, Putkonen M (2011) Advanced process technologies: plasma, direct-write, atmospheric pressure, and roll-to-roll ALD. *MRS Bull* 36:907–913
150. Yin ZP, Huang YA, Bu NB, Wang XM, Xiong YL (2010) Inkjet printing for flexible electronics: materials, processes and equipments. *Chin Sci Bull* 55:3383–3407
151. Street RA, Wong WS, Ready SE, Chabinyc IL, Arias AC, Limb S, Salleo A, Lujan R (2006) Jet printing flexible displays. *Mater Today* 9:32–37
152. Ahn BY, Duoss EB, Motala MJ, Guo XY, Park SI, Xiong YJ, Yoon J, Nuzzo RG, Rogers JA, Lewis JA (2009) Omnidirectional printing of flexible, stretchable, and spanning silver microelectrodes. *Science* 323:1590–1593
153. Muth JT, Vogt DM, Truby RL, Menguc Y, Kolesky DB, Wood RJ, Lewis JA (2014) Embedded 3D printing of strain sensors within highly stretchable elastomers. *Adv Mater* 26:6307–6312
154. Kadekar V, Fang WY, Liou F (2004) Deposition technologies for micromanufacturing: a review. *J Manuf Sci Eng Trans ASME* 126:787–795
155. Arnold CB, Serra P, Pique A (2007) Laser direct-write techniques for printing of complex materials. *MRS Bull* 32:23–31
156. Huang ZM, Zhang YZ, Kotaki M, Ramakrishna S (2003) A review on polymer nanofibers by electrospinning and their applications in nanocomposites. *Compos Sci Technol* 63:2223–2253
157. Li D, Xia YN (2004) Electrospinning of nanofibers: reinventing the wheel? *Adv Mater* 16:1151–1170
158. Chabinyc ML, Wong WS, Arias AC, Ready S, Lujan RA, Daniel JH, Krusor B, Apte RB, Salleo A, Street RA (2005) Printing methods and materials for large-area electronic devices. *Proc IEEE* 93:1491–1499
159. Lee C, Kang H, Kim H, Shin K (2010) Noble logic for preventing scratch on roll-to-roll printed layers in noncontacting transportation. *Jpn J Appl Phys* 49:05EC07
160. Keum H, Carlson A, Ning HL, Mihi A, Eisenhaure JD, Braun PV, Rogers JA, Kim S (2012) Silicon micro-masonry using elastomeric stamps for three-dimensional microfabrication. *J Micromech Microeng* 22:055018
161. Keum H, Chung HJ, Kim S (2013) Electrical contact at the interface between silicon and transfer-printed gold films by eutectic joining. *ACS Appl Mater Interfaces* 5:6061–6065
162. Callister WD (2007) *Materials science and engineering: an introduction*. John Wiley & Sons, New York
163. Lee YY, Lee JH, Cho JY, Kim NR, Nam DH, Choi IS, Nam KT, Joo YC (2013) Stretching-induced growth of PEDOT-rich cores: a new mechanism for strain-dependent resistivity change in PEDOT:PSS films. *Adv Funct Mater* 23:4020–4027
164. Herakovich CT (1981) On the relationship between engineering properties and delamination of composite-materials. *J Compos Mater* 15:336–348
165. Leterrier Y, Pellaton D, Mendels D, Glauser R, Andersons J, Manson JAE (2001) Biaxial fragmentation of thin silicon oxide coatings on poly(ethylene terephthalate). *J Mater Sci* 36:2213–2225. doi:10.1023/A:1017552302379
166. Gleskova H, Cheng IC, Wagner S, Sturm JC, Suo ZG (2006) Mechanics of thin-film transistors and solar cells on flexible substrates. *Sol Energy* 80:687–693
167. Janssen GCAM, Abdalla MM, van Keulen F, Pujada BR, van Venrooy B (2009) Celebrating the 100th anniversary of the Stoney equation for film stress: developments from polycrystalline steel strips to single crystal silicon wafers. *Thin Solid Films* 517:1858–1867
168. Suo Z, Ma EY, Gleskova H, Wagner S (1999) Mechanics of rollable and foldable film-on-foil electronics. *Appl Phys Lett* 74:1177–1179
169. Leterrier Y, Medico L, Demarco F, Manson JAE, Betz U, Escola MF, Olsson MK, Atamny F (2004) Mechanical integrity of transparent conductive oxide films for flexible polymer-based displays. *Thin Solid Films* 460:156–166
170. Vella D, Bico J, Boudaoud A, Roman B, Reis PM (2009) The macroscopic delamination of thin films from elastic substrates. *Proc Natl Acad Sci* 106:10901–10906
171. Kim SR, Nairn JA (2000) Fracture mechanics analysis of coating/substrate systems Part I: analysis of tensile and bending experiments. *Eng Fract Mech* 65:573–593
172. Miller DC, Foster RR, Zhang YD, Jen SH, Bertrand JA, Lu ZX, Seghete D, O’Patches JL, Yang RG, Lee YC, George SM, Dunn ML (2009) The mechanical robustness of atomic-layer- and molecular-layer-deposited coatings on polymer substrates. *J Appl Phys* 105:093527
173. Leterrier Y, Mottet A, Bouquet N, Gillieron D, Dumont P, Pinyol A, Lalande L, Waller JH, Manson JAE (2010) Mechanical integrity of thin inorganic coatings on polymer substrates under quasi-static, thermal and fatigue loadings. *Thin Solid Films* 519:1729–1737
174. Leterrier Y, Andersons J, Pitton Y, Manson JAE (1997) Adhesion of silicon oxide layers on poly(ethylene terephthalate) 2. Effect of coating thickness on adhesive and cohesive strengths. *J Polym Sci B Polym Phys* 35:1463–1472

175. Laws N, Dvorak GJ (1988) Progressive transverse cracking in composite laminates. *J Compos Mater* 22:900–916
176. Sim B, Kim EH, Park J, Lee M (2009) Highly enhanced mechanical stability of indium tin oxide film with a thin Al buffer layer deposited on plastic substrate. *Surf Coat Technol* 204:309–312
177. Park SK, Han JI, Moon DG, Kim WK (2003) Mechanical stability of externally deformed indium-tin-oxide films on polymer substrates. *Jpn J Appl Phys* 42:623–629
178. van der Sluis O, Abdallah AA, Bouten PCP, Timmermans PHM, den Toonder JMJ, de With G (2011) Effect of a hard coat layer on buckle delamination of thin ITO layers on a compliant elastoplastic substrate: an experimental-numerical approach. *Eng Fract Mech* 78:877–889
179. Jia Z, Tucker MB, Li T (2011) Failure mechanics of organic-inorganic multilayer permeation barriers in flexible electronics. *Compos Sci Technol* 71:365–372
180. Wang JS, Sugimura Y, Evans AG, Tredway WK (1998) The mechanical performance of DLC films on steel substrates. *Thin Solid Films* 325:163–174
181. Park JW, Lee SH, Yang CW (2013) Investigation of the interfacial adhesion of the transparent conductive oxide films to large-area flexible polymer substrates using laser-induced thermo-mechanical stresses. *J Appl Phys* 114:063513
182. Park SI, Ahn JH, Feng X, Wang SD, Huang YG, Rogers JA (2008) Theoretical and experimental studies of bending of inorganic electronic materials on plastic substrates. *Adv Funct Mater* 18:2673–2684
183. van der Sluis O, Hsu YY, Timmermans PHM, Gonzalez M, Hoefnagels JPM (2011) Stretching-induced interconnect delamination in stretchable electronic circuits. *J Phys D Appl Phys* 44:034008
184. Chen H, Lu BW, Lin Y, Feng X (2014) Interfacial failure in flexible electronic devices. *IEEE Electron Device Lett* 35:132–134
185. Bruner C, Dauskardt R (2014) Role of molecular weight on the mechanical device properties of organic polymer solar cells. *Macromolecules* 47:1117–1121
186. Brand V, Bruner C, Dauskardt RH (2012) Cohesion and device reliability in organic bulk heterojunction photovoltaic cells. *Sol Energy Mater Sol Cells* 99:182–189
187. Lewis J (2006) Material challenge for flexible organic devices. *Mater Today* 9:38–45
188. Suo ZG (2012) Mechanics of stretchable electronics and soft machines. *MRS Bull* 37:218–225
189. Gleskova H, Wagner S, Suo Z (1999) Failure resistance of amorphous silicon transistors under extreme in-plane strain. *Appl Phys Lett* 75:3011–3013
190. Wu JA, Li M, Chen WQ, Kim DH, Kim YS, Huang YG, Hwang KC, Kang Z, Rogers JA (2010) A strain-isolation design for stretchable electronics. *Acta Mech Sin* 26:881–888
191. Kim DH, Rogers JA (2008) Stretchable electronics: materials strategies and devices. *Adv Mater* 20:4887–4892
192. Bossuyt F, Guenther J, Loher T, Seckel M, Sterken T, de Vries J (2011) Cyclic endurance reliability of stretchable electronic substrates. *Microelectron Reliab* 51:628–635
193. Huyghe B, Rogier H, Vanfleteren J, Axisa F (2008) Design and manufacturing of stretchable high-frequency interconnects. *IEEE Trans Adv Packag* 31:802–808
194. Hsu YY, Papakyrikos C, Liu D, Wang XY, Raj M, Zhang BS, Ghaffari R (2014) Design for reliability of multi-layer stretchable interconnects. *J Micromech Microeng* 24:095014
195. Li T, Suo ZG, Lacour SP, Wagner S (2005) Compliant thin film patterns of stiff materials as platforms for stretchable electronics. *J Mater Res* 20:3274–3277
196. Hsu YY, Lucas K, Davis D, Ghaffari R, Elolampi B, Dalal M, Work J, Lee S, Rafferty C, Dowling K (2013) Design for reliability of multi-layer thin film stretchable interconnects. In: *IEEE 63rd electronic components and technology conference*, pp 623–628
197. Fan JA, Yeo WH, Su YW, Hattori Y, Lee W, Jung SY, Zhang YH, Liu ZJ, Cheng HY, Falgout L, Bajema M, Coleman T, Gregoire D, Larsen RJ, Huang YG, Rogers JA (2014) Fractal design concepts for stretchable electronics. *Nat Commun* 5:3266
198. Rogers JA (2014) Materials for semiconductor devices that can bend, fold, twist, and stretch. *MRS Bull* 39:549–556
199. Khang DY, Rogers JA, Lee HH (2009) Mechanical buckling: mechanics, metrology, and stretchable electronics. *Adv Funct Mater* 19:1526–1536
200. Kim DH, Ahn JH, Choi WM, Kim HS, Kim TH, Song JZ, Huang YGY, Liu ZJ, Lu C, Rogers JA (2008) Stretchable and foldable silicon integrated circuits. *Science* 320:507–511
201. Ko HC, Shin G, Wang SD, Stoykovich MP, Lee JW, Kim DH, Ha JS, Huang YG, Hwang KC, Rogers JA (2009) Curvilinear electronics formed using silicon membrane circuits and elastomeric transfer elements. *Small* 5:2703–2709
202. Sun YG, Choi WM, Jiang HQ, Huang YGY, Rogers JA (2006) Controlled buckling of semiconductor nanoribbons for stretchable electronics. *Nat Nanotechnol* 1:201–207
203. Su YW, Wu J, Fan ZC, Hwang KC, Song JZ, Huang YG, Rogers JA (2012) Postbuckling analysis and its application to stretchable electronics. *J Mech Phys Solids* 60:487–508
204. Choi WM, Song JZ, Khang DY, Jiang HQ, Huang YY, Rogers JA (2007) Biaxially stretchable “wavy” silicon nanomembranes. *Nano Lett* 7:1655–1663
205. Jiang HQ, Khang DY, Song JZ, Sun YG, Huang YG, Rogers JA (2007) Finite deformation mechanics in buckled thin films on compliant supports. *Proc Natl Acad Sci* 104:15607–15612
206. Gorn P, Wagner S (2010) Topographies of plasma-hardened surfaces of poly(dimethylsiloxane). *J Appl Phys* 108:093522
207. Zienkiewicz OC, Taylor RL, Zhu JZ (2013) *The finite element method: its basis and fundamentals*. Elsevier, Oxford
208. Heubner KH, Dewhurst DL, Smith DE, Byrom TG (2001) *The finite element method for engineers*. John Wiley & Sons, New York
209. van der Sluis O, Engelen RAB, Timmermans PHM, Zhang GQ (2009) Numerical analysis of delamination and cracking phenomena in multi-layered flexible electronics. *Microelectron Reliab* 49:853–860
210. Xu W, Lu TJ, Wang F (2010) Effects of interfacial properties on the ductility of polymer-supported metal films for flexible electronics. *Int J Solids Struct* 47:1830–1837
211. Kim DH, Song JZ, Choi WM, Kim HS, Kim RH, Liu ZJ, Huang YY, Hwang KC, Zhang YW, Rogers JA (2008) Materials and noncoplanar mesh designs for integrated circuits with linear elastic responses to extreme mechanical deformations. *Proc Natl Acad Sci* 105:18675–18680
212. Ali A, Hosseini M, Sahari BB (2010) A review of constitutive models for rubber-like materials. *Am J Eng Appl Sci* 3:232–239
213. Liu GR, Quek SS (2013) *The finite element method*. Elsevier, Oxford
214. van Hal BAE, Peerlings RHJ, Geers MGD, van der Sluis OD (2007) Cohesive zone modeling for structural integrity analysis of IC interconnects. *Microelectron Reliab* 47:1251–1261
215. Jin ZH, Sun CT (2006) A comparison of cohesive zone modeling and classical fracture mechanics based on near tip stress field. *Int J Solids Struct* 43:1047–1060
216. ASTM Standard D1709-09 (2009) Impact resistance of plastic film by the free-falling dart method
217. ASTM Standard D3359-09 (2009) Measuring adhesion by tape test
218. ASTM Standard C1624-05 (2009) Adhesion strength and mechanical failure modes of ceramic coatings by quantitative single point scratch testing

219. ASTM Standard D5628-10 (2010) Impact resistance of flat, rigid plastic specimens by means of a falling dart (tup or falling mass)
220. ASTM Standard D5420-10 (2010) Impact resistance of flat, rigid plastic specimen by means of a striker impacted by a falling weight (Gardner impact)
221. ASTM Standard D7187-10 (2010) Measuring mechanistic aspects of scratch/mar behavior of paint coatings by nanoscratching
222. ASTM Standard D7027-13 (2013) Evaluation of scratch resistance of polymeric coatings and plastics using an instrumented scratch machine
223. ASTM Standard E143-13 (2014) Shear modulus at room temperature
224. ASTM Standard D882-12 (2012) Standard test method for tensile properties of thin plastic sheeting
225. Sekitani T, Iba S, Kato Y, Noguchi Y, Someya T, Sakurai T (2005) Ultraflexible organic field-effect transistors embedded at a neutral strain position. *Appl Phys Lett* 87:173502
226. Sokolov AN, Cao YD, Johnson OB, Bao ZA (2012) Mechanistic considerations of bending-strain effects within organic semiconductors on polymer dielectrics. *Adv Funct Mater* 22:175–183
227. Cairns DR, Crawford GP (2005) Electromechanical properties of transparent conducting substrates for flexible electronic displays. *Proc IEEE* 93:1451–1458
228. Fu HR, Xu S, Xu RX, Jiang JQ, Zhang YH, Rogers JA, Huang YG (2015) Lateral buckling and mechanical stretchability of fractal interconnects partially bonded onto an elastomeric substrate. *Appl Phys Lett* 106:091902
229. Janeczek K, Serzysko T, Jakubowska M, Koziol G, Mlozniak A (2012) Mechanical durability of RFID chip joints assembled on flexible substrates. *Solder Surf Mt Technol* 24:206–215
230. Su YW, Li R, Cheng HY, Ying M, Bonifas AP, Hwang KC, Rogers JA, Huang YG (2013) Mechanics of finger-tip electronics. *J Appl Phys* 114:064511
231. Demirci I, Gauthier C, Schirrer R (2005) Mechanical analysis of the damage of a thin polymeric coating during scratching: role of the ratio of the coating thickness to the roughness of a scratching tip. *Thin Solid Films* 479:207–215
232. Chen Z, Wu LYL, Chwa E, Tham O (2008) Scratch resistance of brittle thin films on compliant substrates. *Mater Sci Eng, A* 493:292–298
233. Mittal KL (1976) Adhesion measurement of thin films. *Electrocomp Sci Technol* 3:21–42
234. Volinsky AA, Moody NR, Gerberich WW (2002) Interfacial toughness measurements for thin films on substrates. *Acta Mater* 50:441–466
235. Wang XS, Feng XQ (2002) Effects of thickness on mechanical properties of conducting polythiophene films. *J Mater Sci Lett* 21:715–717
236. Wang XS, Xut JK, Shi GQ, Lu X (2002) Microstructure-mechanical properties relationship in conducting polypyrrole films. *J Mater Sci* 37:5171–5176. doi:10.1023/A:1021093211625
237. Li HC, Rao KK, Jeng JY, Hsiao YJ, Guo TF, Jeng YR, Wen TC (2011) Nano-scale mechanical properties of polymer/fullerene bulk hetero-junction films and their influence on photovoltaic cells. *Sol Energy Mater Sol Cells* 95:2976–2980
238. Chang SY, Hsiao YC, Huang YC (2008) Preparation and mechanical properties of aluminum-doped zinc oxide transparent conducting films. *Surf Coat Technol* 202:5416–5420
239. Saha R, Nix WD (2002) Effects of the substrate on the determination of thin film mechanical properties by nanoindentation. *Acta Mater* 50:23–38
240. Lipomi DJ, Chong H, Vosgueritchian M, Mei JG, Bao ZA (2012) Toward mechanically robust and intrinsically stretchable organic solar cells: evolution of photovoltaic properties with tensile strain. *Sol Energy Mater Sol Cells* 107:355–365
241. Stafford CM, Harrison C, Beers KL, Karim A, Amis EJ, Vandleingham MR, Kim HC, Volksen W, Miller RD, Simonyi EE (2004) A buckling-based metrology for measuring the elastic moduli of polymeric thin films. *Nat Mater* 3:545–550
242. Lang U, Suss T, Dual J (2012) Microtensile testing of submicrometer thick functional polymer samples. *Rev Sci Instrum* 83:075110
243. Tait JG, Worfolk BJ, Maloney SA, Hauger TC, Elias AL, Buriak JM, Harris KD (2013) Spray coated high-conductivity PEDOT:PSS transparent electrodes for stretchable and mechanically-robust organic solar cells. *Sol Energy Mater Sol Cells* 110:98–106
244. Jedaa A, Halik M (2009) Toward strain resistant flexible organic thin film transistors. *Appl Phys Lett* 95:103309
245. Grego S, Lewis J, Vick E, Temple D (2005) Development and evaluation of bend-testing techniques for flexible-display applications. *J Soc Inf Disp* 13:575–581
246. Baumert EK, Pierron ON (2012) Fatigue properties of atomic-layer-deposited alumina ultra-barriers and their implications for the reliability of flexible organic electronics. *Appl Phys Lett* 101:251901
247. Park KI, Lee SY, Kim S, Chang J, Kang SJL, Lee KJ (2010) Bendable and transparent barium titanate capacitors on plastic substrates for high performance flexible ferroelectric devices. *Electrochem Solid-State Lett* 13:G57–G59
248. Ge J, Yao HB, Wang X, Ye YD, Wang JL, Wu ZY, Liu JW, Fan FJ, Gao HL, Zhang CL, Yu SH (2013) Stretchable conductors based on silver nanowires: improved performance through a binary network design. *Angew Chem Int Ed* 52:1654–1659
249. Yu Y, Zeng JF, Chen CJ, Xie Z, Guo RS, Liu ZL, Zhou XC, Yang Y, Zheng ZJ (2014) Three-dimensional compressible and stretchable conductive composites. *Adv Mater* 26:810–815
250. Chou N, Yoo S, Kim S (2012) Fabrication of stretchable and flexible electrodes based on PDMS substrate. In: *IEEE international conference on MEMS*, pp 247–250
251. Lee P, Ham J, Lee J, Hong S, Han S, Suh YD, Lee SE, Yeo J, Lee SS, Lee D, Ko SH (2014) Highly stretchable or transparent conductor fabrication by a hierarchical multiscale hybrid nanocomposite. *Adv Funct Mater* 24:5671–5678
252. Hu LB, Choi JW, Yang Y, Jeong S, La Mantia F, Cui LF, Cui Y (2009) Highly conductive paper for energy-storage devices. *Proc Natl Acad Sci* 106:21490–21494
253. Russo A, Ahn BY, Adams JJ, Duoss EB, Bernhard JT, Lewis JA (2011) Pen-on-paper flexible electronics. *Adv Mater* 23:3426–3430
254. Lee HM, Lee HB, Jung DS, Yun JY, Ko SH, Park SB (2012) Solution Processed Aluminum Paper for Flexible Electronics. *Langmuir* 28:13127–13135
255. Ghosh DS, Chen TL, Formica N, Hwang J, Bruder I, Pruneri V (2012) High figure-of-merit Ag/Al:ZnO nano-thick transparent electrodes for indium-free flexible photovoltaics. *Sol Energy Mater Sol Cells* 107:338–343
256. Lewis J, Grego S, Chalamala B, Vick E, Temple D (2004) Highly flexible transparent electrodes for organic light-emitting diode-based displays. *Appl Phys Lett* 85:3450–3452
257. Alzoubi K, Hamasha MM, Lu SS, Sammakia B (2011) Bending fatigue study of sputtered ITO on flexible substrate. *J Disp Technol* 7:593–600
258. Choi KH, Jeong JA, Kang JW, Kim DG, Kim JK, Na SI, Kim DY, Kim SS, Kim HK (2009) Characteristics of flexible indium tin oxide electrode grown by continuous roll-to-roll sputtering process for flexible organic solar cells. *Sol Energy Mater Sol Cells* 93:1248–1255
259. Park YS, Choi KH, Kim HK (2009) Room temperature flexible and transparent ITO/Ag/ITO electrode grown on flexible PES substrate by continuous roll-to-roll sputtering for flexible organic photovoltaics. *J Phys D Appl Phys* 42:235109

260. Muthukumar A, Giusti G, Jouvert M, Consonni V, Bellet D (2013) Fluorine-doped SnO₂ thin films deposited on polymer substrate for flexible transparent electrodes. *Thin Solid Films* 545:302–309
261. Zeng XY, Zhang QK, Yu RM, Lu CZ (2010) A new transparent conductor: silver nanowire film buried at the surface of a transparent polymer. *Adv Mater* 22:4484–4488
262. Kim KS, Zhao Y, Jang H, Lee SY, Kim JM, Kim KS, Ahn JH, Kim P, Choi JY, Hong BH (2009) Large-scale pattern growth of graphene films for stretchable transparent electrodes. *Nature* 457:706–710
263. Lim JW, Cho DY, Kim J, Na SI, Kim HK (2012) Simple brush-painting of flexible and transparent Ag nanowire network electrodes as an alternative ITO anode for cost-efficient flexible organic solar cells. *Sol Energy Mater Sol Cells* 107:348–354
264. Yu ZB, Zhang QW, Li L, Chen Q, Niu XF, Liu J, Pei QB (2011) Highly flexible silver nanowire electrodes for shape-memory polymer light-emitting diodes. *Adv Mater* 23:664–668
265. Hauger TC, Al-Rafia SMI, Buriak JM (2013) Rolling silver nanowire electrodes: simultaneously addressing adhesion, roughness, and conductivity. *ACS Appl Mater Interfaces* 5:12663–12671
266. De S, Higgins TM, Lyons PE, Doherty EM, Nirmalraj PN, Blau WJ, Boland JJ, Coleman JN (2009) Silver nanowire networks as flexible, transparent, conducting films: extremely high DC to optical conductivity ratios. *ACS Nano* 3:1767–1774
267. Hsu P-C, Kong D, Wang S, Wang H, Welch AJ, Wu H, Cui Y (2014) Electrolessly deposited electrospun metal nanowire transparent electrodes. *J Am Chem Soc* 136:10593–10596
268. Jiu J, Nogi M, Sugahara T, Tokuno T, Araki T, Komoda N, Sugauma K, Uchida H, Shinozaki K (2012) Strongly adhesive and flexible transparent silver nanowire conductive films fabricated with a high-intensity pulsed light technique. *J Mater Chem* 22:23561–23567
269. Guo CF, Sun TY, Liu QH, Suo ZG, Ren ZF (2014) Highly stretchable and transparent nanomesh electrodes made by grain boundary lithography. *Nat Commun* 5:3121
270. Gao TC, Wang BM, Ding B, Lee JK, Leu PW (2014) Uniform and ordered copper nanomeshes by microsphere lithography for transparent electrodes. *Nano Lett* 14:2105–2110
271. Wu H, Hu LB, Rowell MW, Kong DS, Cha JJ, McDonough JR, Zhu J, Yang YA, McGehee MD, Cui Y (2010) Electrospun metal nanofiber webs as high-performance transparent electrode. *Nano Lett* 10:4242–4248
272. Ham J, Kim S, Jung GH, Dong WJ, Lee JL (2013) Design of broadband transparent electrodes for flexible organic solar cells. *J Mater Chem A* 1:3076–3082
273. Gaynor W, Burkhard GF, McGehee MD, Peumans P (2011) Smooth nanowire/polymer composite transparent electrodes. *Adv Mater* 23:2905–2910
274. Chang HX, Wang GF, Yang A, Tao XM, Liu XQ, Shen YD, Zheng ZJ (2010) A transparent, flexible, low-temperature, and solution-processible graphene composite electrode. *Adv Funct Mater* 20:2893–2902
275. De S, Lyons PE, Sorel S, Doherty EM, King PJ, Blau WJ, Nirmalraj PN, Boland JJ, Scardaci V, Joimel J, Coleman JN (2009) Transparent, flexible, and highly conductive thin films based on polymer-nanotube composites. *ACS Nano* 3:714–720
276. Choi DY, Kang HW, Sung HJ, Kim SS (2013) Annealing-free, flexible silver nanowire-polymer composite electrodes via a continuous two-step spray-coating method. *Nanoscale* 5:977–983
277. Lee MS, Lee K, Kim SY, Lee H, Park J, Choi KH, Kim HK, Kim DG, Lee DY, Nam S, Park JU (2013) High-performance, transparent, and stretchable electrodes using graphene-metal nanowire hybrid structures. *Nano Lett* 13:2814–2821
278. Salvatierra RV, Cava CE, Roman LS, Zarbin AJG (2013) ITO-free and flexible organic photovoltaic device based on high transparent and conductive polyaniline/carbon nanotube thin films. *Adv Funct Mater* 23:1490–1499
279. Lee J, Lee P, Lee H, Lee D, Lee SS, Ko SH (2012) Very long Ag nanowire synthesis and its application in a highly transparent, conductive and flexible metal electrode touch panel. *Nanoscale* 4:6408–6414
280. Choi KH, Nam HJ, Jeong JA, Cho SW, Kim HK, Kang JW, Kim DG, Cho WJ (2008) Highly flexible and transparent InZnSnOx/Ag/InZnSnOx multilayer electrode for flexible organic light emitting diodes. *Appl Phys Lett* 92:223302
281. Jing MX, Li M, Chen CY, Wang Z, Shen XQ (2015) Highly bendable, transparent, and conductive AgNWs-PET films fabricated via transfer-printing and second pressing technique. *J Mater Sci* 50:6437–6443. doi:10.1007/s10853-015-9198-3
282. Munzenrieder N, Cherenack KH, Troster G (2011) The effects of mechanical bending and illumination on the performance of flexible IGZO TFTs. *IEEE Trans Electron Devices* 58:2041–2048
283. Sekitani T, Zschieschang U, Klauk H, Someya T (2010) Flexible organic transistors and circuits with extreme bending stability. *Nat Mater* 9:1015–1022
284. Han L, Song K, Mandlik P, Wagner S (2010) Ultraflexible amorphous silicon transistors made with a resilient insulator. *Appl Phys Lett* 96:042111
285. Gleskova H, Wagner S, Soboyejo W, Suo Z (2002) Electrical response of amorphous silicon thin-film transistors under mechanical strain. *J Appl Phys* 92:6224–6229
286. Kuo PC, Jamshidi-Roudbari A, Hatalis M (2009) Electrical characteristics and mechanical limitation of polycrystalline silicon thin film transistor on steel foil under strain. *J Appl Phys* 106:114502
287. Cao Q, Kim HS, Pimparkar N, Kulkarni JP, Wang CJ, Shim M, Roy K, Alam MA, Rogers JA (2008) Medium-scale carbon nanotube thin-film integrated circuits on flexible plastic substrates. *Nature* 454:495–500
288. Loo YL, Someya T, Baldwin KW, Bao ZN, Ho P, Dodabalapur A, Katz HE, Rogers JA (2002) Soft, conformable electrical contacts for organic semiconductors: high-resolution plastic circuits by lamination. *Proc Natl Acad Sci* 99:10252–10256
289. Sekitani T, Iba S, Kato Y, Noguchi Y, Sakurai T, Someya T (2006) Submillimeter radius bendable organic field-effect transistors. *J Non-Cryst Solids* 352:1769–1773
290. Kuo PC, Jamshidi-Roudbari A, Hatalis M (2007) Effect of mechanical strain on mobility of polycrystalline silicon thin-film transistors fabricated on stainless steel foil. *Appl Phys Lett* 91:243507
291. Won SH, Chung JK, Lee CB, Nam HC, Hur JH, Jang J (2004) Effect of mechanical and electrical stresses on the performance of an a-Si: H TFT on plastic substrate. *J Electrochem Soc* 151:G167–G170
292. Servati P, Nathan A (2005) Orientation-dependent strain tolerance of amorphous silicon transistors and pixel circuits for elastic organic light-emitting diode displays. *Appl Phys Lett* 86:033504
293. Ahn JH, Kim HS, Lee KJ, Zhu ZT, Menard E, Nuzzo RG, Rogers JA (2006) High-speed mechanically flexible single-crystal silicon thin-film transistors on plastic substrates. *IEEE Electron Device Lett* 27:460–462
294. Sun L, Qin GX, Seo JH, Celler GK, Zhou WD, Ma ZQ (2010) 12-GHz thin-film transistors on transferrable silicon nanomembranes for high-performance flexible electronics. *Small* 6:2553–2557
295. Lee SK, Jang H, Hasan M, Koo JB, Ahn JH (2010) Mechanically flexible thin film transistors and logic gates on plastic

- substrates by use of single-crystal silicon wires from bulk wafers. *Appl Phys Lett* 96:173501
296. Cao Q, Hur SH, Zhu ZT, Sun YG, Wang CJ, Meitl MA, Shim M, Rogers JA (2006) Highly bendable, transparent thin-film transistors that use carbon-nanotube-based conductors and semiconductors with elastomeric dielectrics. *Adv Mater* 18:304–309
 297. Yu WJ, Lee SY, Chae SH, Perello D, Han GH, Yun M, Lee YH (2011) Small hysteresis nanocarbon-based integrated circuits on flexible and transparent plastic substrate. *Nano Lett* 11:1344–1350
 298. De Arco LG, Zhang Y, Schlenker CW, Ryu K, Thompson ME, Zhou CW (2010) Continuous, highly flexible, and transparent graphene films by chemical vapor deposition for organic photovoltaics. *ACS Nano* 4:2865–2873
 299. Yoon J, Baca AJ, Park SI, Elvikis P, Geddes JB, Li LF, Kim RH, Xiao JL, Wang SD, Kim TH, Motala MJ, Ahn BY, Duoss EB, Lewis JA, Nuzzo RG, Ferreira PM, Huang YG, Rockett A, Rogers JA (2008) Ultrathin silicon solar microcells for semi-transparent, mechanically flexible and microconcentrator module designs. *Nat Mater* 7:907–915
 300. Jiang CY, Sun XW, Tan KW, Lo GQ, Kyaw AKK, Kwong DL (2008) High-bendability flexible dye-sensitized solar cell with a nanoparticle-modified ZnO-nanowire electrode. *Appl Phys Lett* 92:143101
 301. Sun L, Qin GX, Huang H, Zhou H, Behdad N, Zhou WD, Ma ZQ (2010) Flexible high-frequency microwave inductors and capacitors integrated on a polyethylene terephthalate substrate. *Appl Phys Lett* 96:013509
 302. El-Kady MF, Strong V, Dubin S, Kaner RB (2012) Laser scribing of high-performance and flexible graphene-based electrochemical capacitors. *Science* 335:1326–1330
 303. Meng YN, Zhao Y, Hu CG, Cheng HH, Hu Y, Zhang ZP, Shi GQ, Qu LT (2013) All-graphene core-sheath microfibers for all-solid-state, stretchable fibriform supercapacitors and wearable electronic textiles. *Adv Mater* 25:2326–2331
 304. Yang ZB, Deng J, Chen XL, Ren J, Peng HS (2013) A highly stretchable, fiber-shaped supercapacitor. *Angew Chem Int Ed* 52:13453–13457
 305. Chen T, Peng HS, Durstock M, Dai LM (2014) High-performance transparent and stretchable all-solid supercapacitors based on highly aligned carbon nanotube sheets. *Sci Rep* 4:3612
 306. Jost K, Stenger D, Perez CR, McDonough JK, Lian K, Gogotsi Y, Dion G (2013) Knitted and screen printed carbon-fiber supercapacitors for applications in wearable electronics. *Energy Environ Sci* 6:2698–2705
 307. Xu S, Qin Y, Xu C, Wei YG, Yang RS, Wang ZL (2010) Self-powered nanowire devices. *Nat Nanotechnol* 5:366–373
 308. Shepard JF, Chu F, Kanno I, Trolrier-McKinstry S (1999) Characterization and aging response of the d(31) piezoelectric coefficient of lead zirconate titanate thin films. *J Appl Phys* 85:6711–6716
 309. Hiralal P, Imaizumi S, Unalan HE, Matsumoto H, Minagawa M, Rouvala M, Tanioka A, Amaratunga GAJ (2010) Nanomaterial-enhanced all-solid flexible zinc-carbon batteries. *ACS Nano* 4:2730–2734
 310. Gaikwad AM, Chu HN, Qeraj R, Zamarayeva AM, Steingart DA (2013) Reinforced electrode architecture for a flexible battery with paperlike characteristics. *Energy Technol* 1:177–185
 311. Gaikwad AM, Whiting GL, Steingart DA, Arias AC (2011) Highly flexible, printed alkaline batteries based on mesh-embedded electrodes. *Adv Mater* 23:3251–3255
 312. Wang ZQ, Wu ZQ, Bramnik N, Mitra S (2014) Fabrication of high-performance flexible alkaline batteries by implementing multiwalled carbon nanotubes and copolymer separator. *Adv Mater* 26:970–976
 313. Wang ZQ, Bramnik N, Roy S, Di Benedetto G, Zunino JL, Mitra S (2013) Flexible zinc-carbon batteries with multiwalled carbon nanotube/conductive polymer cathode matrix. *J Power Sources* 237:210–214
 314. Noerochim L, Wang JZ, Chou SL, Wexler D, Liu HK (2012) Free-standing single-walled carbon nanotube/SnO₂ anode paper for flexible lithium-ion batteries. *Carbon* 50:1289–1297
 315. Choi KH, Cho SJ, Kim SH, Kwon YH, Kim JY, Lee SY (2014) Thin, deformable, and safety-reinforced plastic crystal polymer electrolytes for high-performance flexible lithium-ion batteries. *Adv Funct Mater* 24:44–52
 316. Liu B, Zhang J, Wang XF, Chen G, Chen D, Zhou CW, Shen GZ (2012) Hierarchical three-dimensional ZnCo₂O₄ nanowire arrays/carbon cloth anodes for a novel class of high-performance flexible lithium-ion batteries. *Nano Lett* 12:3005–3011
 317. Li N, Chen ZP, Ren WC, Li F, Cheng HM (2012) Flexible graphene-based lithium ion batteries with ultrafast charge and discharge rates. *Proc Natl Acad Sci* 109:17360–17365
 318. Kwon YH, Woo SW, Jung HR, Yu HK, Kim K, Oh BH, Ahn S, Lee SY, Song SW, Cho J, Shin HC, Kim JY (2012) Cable-type flexible lithium ion battery based on hollow multi-helix electrodes. *Adv Mater* 24:5192–5197
 319. Koo M, Park KI, Lee SH, Suh M, Jeon DY, Choi JW, Kang K, Lee KJ (2012) Bendable inorganic thin-film battery for fully flexible electronic systems. *Nano Lett* 12:4810–4816
 320. Jeong GS, Baek DH, Jung HC, Song JH, Moon JH, Hong SW, Kim IY, Lee SH (2012) Solderable and electroplatable flexible electronic circuit on a porous stretchable elastomer. *Nat Commun* 3:977
 321. Zhang Z, Guo K, Li Y, Li X, Guan G, Li H, Luo Y, Zhao F, Zhang Q, Wei B, Pei QB, Peng HS (2015) A colour-tunable, weavable fibre-shaped polymer light-emitting electrochemical cell. *Nat Photonics* 9:233–238
 322. Cho H, Yun C, Park JW, Yoo S (2009) Highly flexible organic light-emitting diodes based on ZnS/Ag/WO₃ multilayer transparent electrodes. *Org Electron* 10:1163–1169
 323. Paetzold R, Heuser K, Henseler D, Roeger S, Wittmann G, Winkler A (2003) Performance of flexible polymeric light-emitting diodes under bending conditions. *Appl Phys Lett* 82:3342–3344
 324. Han TH, Lee Y, Choi MR, Woo SH, Bae SH, Hong BH, Ahn JH, Lee TW (2012) Extremely efficient flexible organic light-emitting diodes with modified graphene anode. *Nat Photonics* 6:105–110
 325. Li L, Yu ZB, Hu WL, Chang CH, Chen Q, Pei QB (2011) Efficient flexible phosphorescent polymer light-emitting diodes based on silver nanowire-polymer composite electrode. *Adv Mater* 23:5563–5567
 326. Lee CH, Kim YJ, Hong YJ, Jeon SR, Bae S, Hong BH, Yi GC (2011) Flexible inorganic nanostructure light-emitting diodes fabricated on graphene films. *Adv Mater* 23:4614–4619
 327. Lee SY, Park KI, Huh C, Koo M, Yoo HG, Kim S, Ah CS, Sung GY, Lee KJ (2012) Water-resistant flexible GaN LED on a liquid crystal polymer substrate for implantable biomedical applications. *Nano Energy* 1:145–151
 328. Yun J, Cho K, Park B, Park BH, Kim S (2009) Resistance switching memory devices constructed on plastic with solution-processed titanium oxide. *J Mater Chem* 19:2082–2085
 329. Yu AD, Kurosawa T, Lai YC, Higashihara T, Ueda M, Liu CL, Chen WC (2012) Flexible polymer memory devices derived from triphenylamine-pyrene containing donor-acceptor polyimides. *J Mater Chem* 22:20754–20763
 330. Zhou Y, Han ST, Xu ZX, Roy VAL (2012) Low voltage flexible nonvolatile memory with gold nanoparticles embedded in poly(methyl methacrylate). *Nanotechnology* 23:344014
 331. Zhou Y, Han ST, Xu ZX, Roy VAL (2013) The strain and thermal induced tunable charging phenomenon in low power

- flexible memory arrays with a gold nanoparticle monolayer. *Nanoscale* 5:1972–1979
332. Jung S, Kong J, Song S, Lee K, Lee T, Hwang H, Jeon S (2011) Flexible resistive random access memory using solution-processed TiOx with Al top electrode on Ag layer-inserted indium-zinc-tin-oxide-coated polyethersulfone substrate. *Appl Phys Lett* 99:142110
 333. Ji Y, Lee S, Cho B, Song S, Lee T (2011) Flexible organic memory devices with multilayer graphene electrodes. *ACS Nano* 5:5995–6000
 334. Kim SM, Song EB, Lee S, Zhu JF, Seo DH, Mecklenburg M, Seo S, Wang KL (2012) Transparent and flexible graphene charge-trap memory. *ACS Nano* 6:7879–7884
 335. Kim S, Jeong HY, Kim SK, Choi SY, Lee KJ (2011) Flexible memristive memory array on plastic substrates. *Nano Lett* 11:5438–5442
 336. Jeong HY, Kim JY, Kim JW, Hwang JO, Kim JE, Lee JY, Yoon TH, Cho BJ, Kim SO, Ruoff RS, Choi SY (2010) Graphene oxide thin films for flexible nonvolatile memory applications. *Nano Lett* 10:4381–4386
 337. Kim SJ, Lee JS (2010) Flexible organic transistor memory devices. *Nano Lett* 10:2884–2890
 338. Hwang SK, Bae I, Kim RH, Park C (2012) Flexible non-volatile ferroelectric polymer memory with gate-controlled multilevel operation. *Adv Mater* 24:5910–5914
 339. Yu WJ, Chae SH, Lee SY, Duong DL, Lee YH (2011) Ultra-transparent, flexible single-walled carbon nanotube non-volatile memory device with an oxygen-decorated graphene electrode. *Adv Mater* 23:1889–1893
 340. Ji Y, Cho B, Song S, Kim TW, Choe M, Kahng YH, Lee T (2010) Stable switching characteristics of organic nonvolatile memory on a bent flexible substrate. *Adv Mater* 22:3071–3075
 341. Kim WY, Lee HC (2012) Stable ferroelectric poly(vinylidene fluoride-trifluoroethylene) film for flexible nonvolatile memory application. *IEEE Electron Device Lett* 33:260–262
 342. Lee S, Kim H, Yun DJ, Rhee SW, Yong K (2009) Resistive switching characteristics of ZnO thin film grown on stainless steel for flexible nonvolatile memory devices. *Appl Phys Lett* 95:262113
 343. Lee MH, Yun DY, Park HM, Kim TW (2011) Flexible organic bistable devices based on [6,6]-phenyl-C85 butyric acid methyl ester clusters embedded in a polymethyl methacrylate layer. *Appl Phys Lett* 99:183301
 344. Han ST, Zhou Y, Xu ZX, Huang LB, Yang XB, Roy VAL (2012) Microcontact printing of ultrahigh density gold nanoparticle monolayer for flexible flash memories. *Adv Mater* 24:3556–3561
 345. Jun JH, Cho K, Yun J, Kim S (2011) Switching memory cells constructed on plastic substrates with silver selenide nanoparticles. *J Mater Sci* 46:6767–6771. doi:10.1007/s10853-011-5633-2
 346. Sierros KA, Hecht DS, Banerjee DA, Morris NJ, Hu L, Irvin GC, Lee RS, Cairns DR (2010) Durable transparent carbon nanotube films for flexible device components. *Thin Solid Films* 518:6977–6983
 347. Takamatsu S, Takahata T, Muraki M, Iwase E, Matsumoto K, Shimoyama I (2010) Transparent conductive-polymer strain sensors for touch input sheets of flexible displays. *J Micromech Microeng* 20:075017
 348. Wang J, Liang MH, Fang Y, Qiu TF, Zhang J, Zhi LJ (2012) Rod-coating: towards large-area fabrication of uniform reduced graphene oxide films for flexible touch screens. *Adv Mater* 24:2874–2878
 349. ten Cate AT, Gaspar CH, Virtanen HLK, Stevens RSA, Koldewij RBJ, Olkkonen JT, Rentrop CHA, Smolander MH (2014) Printed electronic switch on flexible substrates using printed microcapsules. *J Mater Sci* 49:5831–5837. doi:10.1007/s10853-014-8271-7
 350. Lin CP, Chang CH, Cheng YT, Jou CF (2011) Development of a flexible SU-8/PDMS-based antenna. *IEEE Antennas Wirel Propag Lett* 10:1108–1111
 351. Khaleel HR, Al-Rizzo HM, Rucker DG, Mohan S (2012) A compact polyimide-based UWB antenna for flexible electronics. *IEEE Antennas Wirel Propag Lett* 11:564–567
 352. Chameswary J, Sebastian MT (2015) Preparation and properties of BaTiO3 filled butyl rubber composites for flexible electronic circuit applications. *J Mater Sci* 26:4629–4637. doi:10.1007/s10854-015-2879-5
 353. Graz IM, Lacour SP (2009) Flexible pentacene organic thin film transistor circuits fabricated directly onto elastic silicone membranes. *Appl Phys Lett* 95:243305
 354. Xu F, Zhu Y (2012) Highly conductive and stretchable silver nanowire conductors. *Adv Mater* 24:5117–5122
 355. Das NC, Chaki TK, Khastgir D (2002) Effect of axial stretching on electrical resistivity of short carbon fibre and carbon black filled conductive rubber composites. *Polym Int* 51:156–163
 356. Hansen TS, West K, Hassager O, Larsen NB (2007) Highly stretchable and conductive polymer material made from poly(3,4-ethylenedioxythiophene) and polyurethane elastomers. *Adv Funct Mater* 17:3069–3073
 357. Oh KW, Park HJ, Kim SH (2003) Stretchable conductive fabric for electrotherapy. *J Appl Polym Sci* 88:1225–1229
 358. Hsu YY, Gonzalez M, Bossuyt F, Vanfleteren J, De Wolf I (2011) Polyimide-enhanced stretchable interconnects: design, fabrication, and characterization. *IEEE Trans Electron Devices* 58:2680–2688
 359. Yu ZB, Niu XF, Liu ZT, Pei QB (2011) Intrinsically stretchable polymer light-emitting devices using carbon nanotube-polymer composite electrodes. *Adv Mater* 23:3989–3994
 360. Sekitani T, Noguchi Y, Hata K, Fukushima T, Aida T, Someya T (2008) A rubberlike stretchable active matrix using elastic conductors. *Science* 321:1468–1472
 361. Lee P, Lee J, Lee H, Yeo J, Hong S, Nam KH, Lee D, Lee SS, Ko SH (2012) Highly stretchable and highly conductive metal electrode by very long metal nanowire percolation network. *Adv Mater* 24:3326–3332
 362. Graz IM, Cotton DPJ, Lacour SP (2009) Extended cyclic uniaxial loading of stretchable gold thin-films on elastomeric substrates. *Appl Phys Lett* 94:071902
 363. Bossuyt F, Vervust T, Vanfleteren J (2013) Stretchable electronics technology for large area applications: fabrication and mechanical characterization. *IEEE Trans Compon Packag Manuf Technol* 3:229–235
 364. Akter T, Kim WS (2012) Reversibly stretchable transparent conductive coatings of spray-deposited silver nanowires. *ACS Appl Mater Interfaces* 4:1855–1859
 365. Lipomi DJ, Lee JA, Vosgueritchian M, Tee BCK, Bolander JA, Bao ZA (2012) Electronic properties of transparent conductive films of PEDOT:PSS on stretchable substrates. *Chem Mater* 24:373–382
 366. Hauger TC, Zeberoff A, Worfolk BJ, Elias AL, Harris KD (2014) Real-time resistance, transmission and figure-of-merit analysis for transparent conductors under stretching-mode strain. *Sol Energy Mater Sol Cells* 124:247–255
 367. Keplinger C, Sun JY, Foo CC, Rothmund P, Whitesides GM, Suo ZG (2013) Stretchable, transparent, ionic conductors. *Science* 341:984–987
 368. Cairns DR, Witte RP, Sparacin DK, Sachsman SM, Paine DC, Crawford GP, Newton RR (2000) Strain-dependent electrical resistance of tin-doped indium oxide on polymer substrates. *Appl Phys Lett* 76:1425–1427

369. Azar AD, Finley E, Harris KD (2015) Instrument for evaluating the electrical resistance and wavelength-resolved transparency of stretchable electronics during strain. *Rev Sci Instrum* 86:013901
370. Kaltenbrunner M, White MS, Glowacki ED, Sekitani T, Someya T, Sariciftci NS, Bauer S (2012) Ultrathin and lightweight organic solar cells with high flexibility. *Nat Commun* 3:770
371. Lee J, Wu JA, Shi MX, Yoon J, Park SI, Li M, Liu ZJ, Huang YG, Rogers JA (2011) Stretchable GaAs photovoltaics with designs that enable high areal coverage. *Adv Mater* 23:986–991
372. Lipomi DJ, Tee BCK, Vosgueritchian M, Bao ZN (2011) Stretchable organic solar cells. *Adv Mater* 23:1771–1775
373. Yang ZB, Deng J, Sun XM, Li HP, Peng HS (2014) Stretchable, wearable dye-sensitized solar cells. *Adv Mater* 26:2643–2647
374. Graz IM, Cotton DPJ, Robinson A, Lacour SP (2011) Silicone substrate with in situ strain relief for stretchable thin-film transistors. *Appl Phys Lett* 98:124101
375. Khang DY, Jiang HQ, Huang Y, Rogers JA (2006) A stretchable form of single-crystal silicon for high-performance electronics on rubber substrates. *Science* 311:208–212
376. Kaltenbrunner M, Sekitani T, Reeder J, Yokota T, Kuribara K, Tokuhara T, Drack M, Schwodiauer R, Graz I, Bauer-Gogonea S, Bauer S, Someya T (2013) An ultra-lightweight design for imperceptible plastic electronics. *Nature* 499:458–463
377. Someya T, Kato Y, Sekitani T, Iba S, Noguchi Y, Murase Y, Kawaguchi H, Sakurai T (2005) Conformable, flexible, large-area networks of pressure and thermal sensors with organic transistor active matrixes. *Proc Natl Acad Sci* 102:12321–12325
378. Chae SH, Yu WJ, Bae JJ, Duong DL, Perello D, Jeong HY, Ta QH, Ly TH, Vu QA, Yun M, Duan XF, Lee YH (2013) Transferred wrinkled Al₂O₃ for highly stretchable and transparent graphene-carbon nanotube transistors. *Nat Mater* 12:403–409
379. Yu CJ, Masarapu C, Rong JP, Wei BQ, Jiang HQ (2009) Stretchable supercapacitors based on buckled single-walled carbon nanotube macrofilms. *Adv Mater* 21:4793–4797
380. Chen T, Hao R, Peng HS, Dai LM (2015) High-performance, stretchable, wire-shaped supercapacitors. *Angew Chem Int Ed* 54:618–622
381. Kim D, Shin G, Kang YJ, Kim W, Ha JS (2013) Fabrication of a stretchable solid-state micro-supercapacitor array. *ACS Nano* 7:7975–7982
382. Niu ZQ, Dong HB, Zhu BW, Li JZ, Hng HH, Zhou WY, Chen XD, Xie SS (2013) Highly stretchable, integrated supercapacitors based on single-walled carbon nanotube films with continuous reticulate architecture. *Adv Mater* 25:1058–1064
383. Yue BB, Wang CY, Ding X, Wallace GG (2012) Polypyrrole coated nylon lycra fabric as stretchable electrode for supercapacitor applications. *Electrochim Acta* 68:18–24
384. Yun TG, Oh M, Hu LB, Hyun S, Han SM (2013) Enhancement of electrochemical performance of textile based supercapacitor using mechanical pre-straining. *J Power Sources* 244:783–791
385. Chen T, Xue YH, Roy AK, Dai LM (2014) Transparent and stretchable high-performance supercapacitors based on wrinkled graphene electrodes. *ACS Nano* 8:1039–1046
386. Gaikwad AM, Zamarayeva AM, Rousseau J, Chu HW, Derin I, Steingart DA (2012) Highly stretchable alkaline batteries based on an embedded conductive fabric. *Adv Mater* 24:5071–5076
387. Kaltenbrunner M, Kettlgruber G, Siket C, Schwodiauer R, Bauer S (2010) Arrays of ultracompliant electrochemical dry gel cells for stretchable electronics. *Adv Mater* 22:2065–2067
388. Kettlgruber G, Kaltenbrunner M, Siket CM, Moser R, Graz IM, Schwodiauer R, Bauer S (2013) Intrinsically stretchable and rechargeable batteries for self-powered stretchable electronics. *J Mater Chem A* 1:5505–5508
389. Wang CY, Zheng W, Yue ZL, Too CO, Wallace GG (2011) Buckled, stretchable polypyrrole electrodes for battery applications. *Adv Mater* 23:3580–3584
390. Yan CY, Wang X, Cui MQ, Wang JX, Kang WB, Foo CY, Lee PS (2014) Stretchable silver-zinc batteries based on embedded nanowire elastic conductors. *Adv Energy Mater* 4:1301396
391. Zhu GA, Yang RS, Wang SH, Wang ZL (2010) Flexible high-output nanogenerator based on lateral ZnO nanowire array. *Nano Lett* 10:3151–3155
392. Liang JJ, Li L, Niu XF, Yu ZB, Pei QB (2013) Elastomeric polymer light-emitting devices and displays. *Nat Photonics* 7:817–824
393. So JH, Thelen J, Qusba A, Hayes GJ, Lazzi G, Dickey MD (2009) Reversibly deformable and mechanically tunable fluidic antennas. *Adv Funct Mater* 19:3632–3637
394. Cheng S, Wu ZG (2010) Microfluidic stretchable RF electronics. *Lab Chip* 10:3227–3234
395. Huang YA, Wang YZ, Xiao L, Liu HM, Dong WT, Yin ZP (2014) Microfluidic serpentine antennas with designed mechanical tunability. *Lab Chip* 14:4205–4212
396. Park M, Im J, Shin M, Min Y, Park J, Cho H, Park S, Shim MB, Jeon S, Chung DY, Bae J, Park J, Jeong U, Kim K (2012) Highly stretchable electric circuits from a composite material of silver nanoparticles and elastomeric fibres. *Nat Nanotechnol* 7:803–809
397. Cheng S, Rydberg A, Hjort K, Wu ZG (2009) Liquid metal stretchable unbalanced loop antenna. *Appl Phys Lett* 94:144103
398. Song LN, Myers AC, Adams JJ, Zhu Y (2014) Stretchable and reversibly deformable radio frequency antennas based on silver nanowires. *ACS Appl Mater Interfaces* 6:4248–4253
399. Cheng S, Wu ZG, Hallbjorner P, Hjort K, Rydberg A (2009) Foldable and stretchable liquid metal planar inverted cone antenna. *IEEE Trans Antennas Propag* 57:3765–3771
400. Jeong SH, Hagman A, Hjort K, Jobs M, Sundqvist J, Wu ZG (2012) Liquid alloy printing of microfluidic stretchable electronics. *Lab Chip* 12:4657–4664
401. Li MFF, Li HY, Zhong WB, Zhao QH, Wang D (2014) Stretchable conductive polypyrrole/polyurethane (PPy/PU) strain sensor with netlike microcracks for human breath detection. *ACS Appl Mater Interfaces* 6:1313–1319
402. Lee YC, Liu TS (2014) Deformation of multilayer flexible electronics subjected to torque. *Exp Tech* 38:13–20
403. Lederman SJ, Taylor MM (1972) Fingertip force, surface geometry, and perception of roughness by active touch. *Percept Psychophys* 12:401–408
404. Zysset C, Kinkeldei TW, Munzenrieder N, Cherenack K, Troster G (2012) Integration method for electronics in woven textiles. *IEEE Trans Compon Packag Manuf Technol* 2:1107–1117
405. Su Y, Wu J, Fan Z, Hwang K-C, Huang Y, Rogers JA (2013) Mechanics of twistable electronics. *Stretchable Electronics*. Wiley-VCH, Weinheim, pp 31–39
406. Chen Q, Xu L, Salo A, Neto G, Freitas G (2008) Reliability study of flexible display module by experiments. *Int Conf Electron Packag Technol High Density Packag* 1–2:1086–1091
407. Chen Q, Xu L, Salo A, Neto G, Freitas G (2008) Reliability of flexible display by simulation and strain gauge test. In: 10th electronics packaging technology conference 1–3, pp 322–327
408. Zeberoff A (2013) Remote activation of a microactuator using a photo-responsive nanoparticle-polymer composite. M.Sc. Thesis, University of Alberta
409. Cordill MJ, Bahr DF, Moody NR, Gerberich WW (2004) Recent developments in thin film adhesion measurement. *IEEE Trans Device Mater Reliab* 4:163–168
410. Zhu R, Chung CH, Cha KC, Yang WB, Zheng YB, Zhou HP, Song TB, Chen CC, Weiss PS, Li G, Yang Y (2011) Fused silver nanowires with metal oxide nanoparticles and organic polymers for highly transparent conductors. *ACS Nano* 5:9877–9882
411. Liu CH, Yu X (2011) Silver nanowire-based transparent, flexible, and conductive thin film. *Nanoscale Res Lett* 6:75
412. Li XK, Gittleson F, Carmo M, Sekol RC, Taylor AD (2012) Scalable fabrication of multifunctional freestanding carbon

- nanotube/polymer composite thin films for energy conversion. *ACS Nano* 6:1347–1356
413. Gaikwad AM, Steingart DA, Ng TN, Schwartz DE, Whiting GL (2013) A flexible high potential printed battery for powering printed electronics. *Appl Phys Lett* 102:233302
 414. Covarel G, Bensaid B, Boddaert X, Giljean S, Benaben P, Louis P (2012) Characterization of organic ultra-thin film adhesion on flexible substrate using scratch test technique. *Surf Coat Technol* 211:138–142
 415. Amendola E, Cammarano A, Pezzuto M, Acierno D (2009) Adhesion of functional layer on polymeric substrates for optoelectronic applications. *J Eur Opt Soc* 4:09027
 416. Dupont SR, Novoa F, Voroshazi E, Dauskardt RH (2014) Decohesion kinetics of PEDOT:PSS conducting polymer films. *Adv Funct Mater* 24:1325–1332
 417. Dupont SR, Voroshazi E, Heremans P, Dauskardt RH (2013) Adhesion properties of inverted polymer solar cells: processing and film structure parameters. *Org Electron* 14:1262–1270
 418. Dupont SR, Oliver M, Krebs FC, Dauskardt RH (2012) Interlayer adhesion in roll-to-roll processed flexible inverted polymer solar cells. *Sol Energy Mater Sol Cells* 97:171–175
 419. Sierros KA, Banerjee DA, Morris NJ, Cairns DR, Kortidis I, Kiriakidis G (2010) Mechanical properties of ZnO thin films deposited on polyester substrates used in flexible device applications. *Thin Solid Films* 519:325–330
 420. Liu ZH, Pan CT, Chen YC, Liang PH (2013) Interfacial characteristics of polyethylene terephthalate-based piezoelectric multi-layer films. *Thin Solid Films* 531:284–293
 421. Liu Y, Guo C-F, Huang S, Sun T, Wang Y, Ren Z (2015) A new method for fabricating ultrathin metal films as scratch-resistant flexible transparent electrodes. *J Mater Sci* 1:52–59
 422. Huang Y, Feng X, Qu BR (2011) Slippage toughness measurement of soft interface between stiff thin films and elastomeric substrate. *Rev Sci Instrum* 82:104704
 423. Tummala NR, Bruner C, Risko C, Bredas J-L, Dauskardt RH (2015) Molecular-scale understanding of cohesion and fracture in P3HT:fullerene blends. *ACS Appl Mater Interfaces* 7:9957–9964
 424. Islam RA, Chan YC, Ralph B (2004) Effect of drop impact energy on contact resistance of anisotropic conductive adhesive film joints. *J Mater Res* 19:1662–1668
 425. Yanaka M, Tsukahara Y, Nakaso N, Takeda N (1998) Cracking phenomena of brittle films in nanostructure composites analysed by a modified shear lag model with residual strain. *J Mater Sci* 33:2111–2119. doi:10.1023/A:1004371203514
 426. Rogers JA, Lagally MG, Nuzzo RG (2011) Synthesis, assembly and applications of semiconductor nanomembranes. *Nature* 477:45–53
 427. Roberts MM, Klein LJ, Savage DE, Slinker KA, Friesen M, Celler G, Eriksson MA, Lagally MG (2006) Elastically relaxed free-standing strained-silicon nanomembranes. *Nat Mater* 5:388–393
 428. Li XL (2008) Strain induced semiconductor nanotubes: from formation process to device applications. *J Phys D Appl Phys* 41:193001
 429. Prinz VY, Seleznev VA, Gutakovskiy AK, Chehovskiy AV, Preobrazhenskii VV, Putyato MA, Gavrilova TA (2000) Free-standing and overgrown InGaAs/GaAs nanotubes, nanohelices and their arrays. *Physica E* 6:828–831
 430. Schmidt OG, Eberl K (2001) Nanotechnology—thin solid films roll up into nanotubes. *Nature* 410:168
 431. Rogers JA, Huang YG (2009) A curvy, stretchy future for electronics. *Proc Natl Acad Sci* 106:10875–10876
 432. Mei HX, Huang R, Chung JY, Stafford CM, Yu HH (2007) Buckling modes of elastic thin films on elastic substrates. *Appl Phys Lett* 90:151902
 433. Feng X, Yang BD, Liu YM, Wang Y, Dagdeviren C, Liu ZJ, Carlson A, Li JY, Huang YG, Rogers JA (2011) Stretchable ferroelectric nanoribbons with wavy configurations on elastomeric substrates. *ACS Nano* 5:3326–3332
 434. Duan XF, Niu CM, Sahi V, Chen J, Parce JW, Empedocles S, Goldman JL (2003) High-performance thin-film transistors using semiconductor nanowires and nanoribbons. *Nature* 425:274–278
 435. Bertolazzi S, Krasnozhan D, Kis A (2013) Nonvolatile memory cells based on MoS₂/graphene heterostructures. *ACS Nano* 7:3246–3252
 436. Eda G, Fanchini G, Chhowalla M (2008) Large-area ultrathin films of reduced graphene oxide as a transparent and flexible electronic material. *Nat Nanotechnol* 3:270–274
 437. Lee J, Wu J, Ryu JH, Liu ZJ, Meitl M, Zhang YW, Huang YG, Rogers JA (2012) Stretchable semiconductor technologies with high areal coverages and strain-limiting behavior: demonstration in high-efficiency dual-junction GaInP/GaAs photovoltaics. *Small* 8:1851–1856
 438. Rogers JA, Someya T, Huang YG (2010) Materials and mechanics for stretchable electronics. *Science* 327:1603–1607
 439. Lacour SP, Wagner S, Narayan RJ, Li T, Suo ZG (2006) Stiff subcircuit islands of diamondlike carbon for stretchable electronics. *J Appl Phys* 100:014913
 440. Aarts AAA, Srivannavit O, Wise KD, Yoon E, Puers R, Van Hoof C, Neves HP (2011) Fabrication technique of a compressible biocompatible interconnect using a thin film transfer process. *J Micromech Microeng* 21:074012
 441. Vanfleteren J, Gonzalez M, Bossuyt F, Hsu YY, Vervust T, De Wolf I, Jablonski M (2012) Printed circuit board technology inspired stretchable circuits. *MRS Bull* 37:254–260
 442. Tian BZ, Liu J, Dvir T, Jin LH, Tsui JH, Qing Q, Suo ZG, Langer R, Kohane DS, Lieber CM (2012) Macroporous nanowire nanoelectronic scaffolds for synthetic tissues. *Nat Mater* 11:986–994
 443. Sun JY, Zhao XH, Illeperuma WRK, Chaudhuri O, Oh KH, Mooney DJ, Vlassak JJ, Suo ZG (2012) Highly stretchable and tough hydrogels. *Nature* 489:133–136